

# DO I KNOW THIS ENTITY? KNOWLEDGE AWARENESS AND HALLUCINATIONS IN LANGUAGE MODELS

**Anonymous authors**

Paper under double-blind review

## ABSTRACT

Hallucinations in large language models are a widespread problem, yet the mechanisms behind whether models will hallucinate are poorly understood, limiting our ability to solve this problem. Using sparse autoencoders as an interpretability tool, we discover that a key part of these mechanisms is *entity recognition*, where the model detects if an entity is one it can recall facts about. Sparse autoencoders uncover meaningful directions in the representation space, these detect whether the model recognizes an entity, e.g. detecting it doesn't know about an athlete or a movie. This suggests that models **might** have self-knowledge: internal representations about their own capabilities. These directions are causally relevant: capable of steering the model to refuse to answer questions about known entities, or to hallucinate attributes of unknown entities when it would otherwise refuse. We demonstrate that despite the sparse autoencoders being trained on the base model, these directions have a causal effect on the chat model's refusal behavior, suggesting that chat finetuning has repurposed this existing mechanism. Furthermore, we provide an initial exploration into the mechanistic role of these directions in the model, finding that they disrupt the attention of downstream heads that typically move entity attributes to the final token.

## 1 INTRODUCTION

Large Language Models (LLMs) have remarkable capabilities (Radford et al., 2019; Brown et al., 2020; Hoffmann et al., 2022; Chowdhery et al., 2023) yet have a propensity to hallucinate: generating text that is fluent but factually incorrect or unsupported by available information (Ji et al., 2023; Minaee et al., 2024). This significantly limits their application in real-world settings where factuality is crucial, such as healthcare. Despite the prevalence and importance of this issue, the mechanistic understanding of whether LLMs will hallucinate on a given prompt remains limited. While there has been much work interpreting factual recall (Geva et al., 2023; Nanda et al., 2023; Chughtai et al., 2024; Yu et al., 2023), it has mainly focused on the mechanism behind recalling known facts, not on hallucinations or refusals to answer, leaving a significant gap in our understanding.

Language models can produce hallucinations due to various factors, including flawed data sources or outdated factual knowledge (Huang et al., 2023). However, an important subset of hallucinations occurs when models are prompted to generate information they don't possess. We operationalize this phenomenon by considering queries about entities of different types (movies, cities, players, and songs). Given a question about an unknown entity, the model either hallucinates or refuses to answer. In this work, we find linear directions in the representation space that **potentially encode a form of self-knowledge**: assessing their own knowledge or lack thereof regarding specific entities. These directions are causally relevant for whether it refuses to answer. We note that the existence of this kind of **knowledge awareness** does not necessarily imply the existence of other forms of self-knowledge, and may be specific to the factual recall mechanism.

We find these directions using Sparse Autoencoders (SAEs) (Bricken et al., 2023; Cunningham et al., 2023). SAEs are an interpretability tool for finding a sparse, interpretable decomposition of model representations. They are motivated by the Linear Representation Hypothesis (Park et al., 2023; Mikolov et al., 2013): that interpretable properties of the input (features) such as sentiment (Tigges et al., 2023) or truthfulness (Li et al., 2023; Zou et al., 2023) are encoded as linear directions in the representation space, and that model representations are sparse linear combinations of these

054  
055  
056  
057  
058  
059  
060  
061  
062  
063  
064  
065  
066  
067  
068  
069  
070  
071  
072  
073  
074  
075  
076  
077  
078  
079  
080  
081  
082  
083  
084  
085  
086  
087  
088  
089  
090  
091  
092  
093  
094  
095  
096  
097  
098  
099  
100  
101  
102  
103  
104  
105  
106  
107

Known Entity Latent Activations	Unknown Entity Latent Activations
Michael <b>Jordan</b>	Michael <b>Joordan</b>
When was the player <b>LeBron James</b> born?	When was the player Wilson <b>Brown</b> born?
He was born in the city of <b>San Francisco</b>	He was born in the city of <b>Anthon</b>
I just watched the movie 12 <b>Angry Men</b>	I just watched the movie 20 <b>Angry Men</b>
The <b>Beatles</b> song ‘Yellow <b>Submarine</b> ’	The Beatles song ‘ <b>Turquoise Submarine</b> ’

Table 1: Pair of sparse autoencoder latents that activate on known (left) and unknown entities (right) respectively. They fire consistently across entity types (movies, cities, songs, and players).

directions. We use Gemma Scope (Lieberum et al., 2024), which offers a suite of SAEs trained on every layer of Gemma 2 models (Team et al., 2024), and find internal representations [that suggest to encode knowledge awareness](#) in Gemma 2 2B and 9B.

Arditi et al. (2024) discovered that the decision to refuse a harmful request is mediated by a single direction. Building on this work, we demonstrate that a model’s refusal to answer requests about attributes of entities (*knowledge refusal*) can similarly be steered with our found entity recognition directions. This finding is particularly intriguing given that Gemma Scope SAEs were trained on the base model on pre-training data. Yet, SAE-derived directions have a causal effect on knowledge-based refusal in the chat model—a behavior incentivized in the finetuning stage. This insight provides additional evidence for the hypothesis that finetuning often repurposes existing mechanisms (Jain et al., 2024; Prakash et al., 2024; Kissane et al., 2024).

Overall, our contributions are as follows:

- Using sparse autoencoders (SAEs) we **discover directions in the representation space on the final token of an entity, detecting whether the model can recall facts about the entity, suggesting they encode a form of knowledge awareness.**
- Our findings show that **entity recognition directions generalize across diverse entity types:** players, films, songs, cities, and more.
- We demonstrate that these directions **causally affect knowledge refusal in the chat model**, i.e. by steering with these directions, we can cause the model to hallucinate rather than refuse on unknown entities, and refuse to answer questions about known entities.
- We find that **unknown entity recognition directions disrupt the factual recall mechanism**, by suppressing the attention of attribute extraction heads, shown in prior work (Nanda et al., 2023; Geva et al., 2023) to be a key part of the mechanism.
- We go beyond merely understanding knowledge refusal, and find **SAE latents, seemingly representing uncertainty, that are predictive of incorrect answers.**

## 2 SPARSE AUTOENCODERS

Dictionary learning (Olshausen & Field, 1997) offers a powerful approach for disentangling features in superposition. Sparse Autoencoders (SAEs) have proven to be effective for this task (Sharkey et al., 2022; Bricken et al., 2023). SAEs project model representations  $\mathbf{x} \in \mathbb{R}^d$  into a larger dimensional space  $a(\mathbf{x}) \in \mathbb{R}^{d_{SAE}}$ . In this work, we use the SAEs from Gemma Scope (Lieberum et al., 2024)<sup>1</sup>, which use the JumpReLU SAE architecture (Rajamanoharan et al., 2024), which defines the function

$$\text{SAE}(\mathbf{x}) = a(\mathbf{x})\mathbf{W}_{\text{dec}} + \mathbf{b}_{\text{dec}}, \quad (1)$$

where

$$a(\mathbf{x}) = \text{JumpReLU}_{\theta}(\mathbf{x}\mathbf{W}_{\text{enc}} + \mathbf{b}_{\text{enc}}), \quad (2)$$

with the activation function (Erichson et al., 2019)  $\text{JumpReLU}_{\theta}(\mathbf{x}) = \mathbf{x} \odot H(\mathbf{x} - \theta)$ , composed by  $H$ , the Heaviside step function, and  $\theta$ , a learnable vector acting as a threshold. Intuitively, this is

<sup>1</sup>We use the default sparsity for each layer, the ones available in Neuronpedia (Lin & Bloom, 2024).

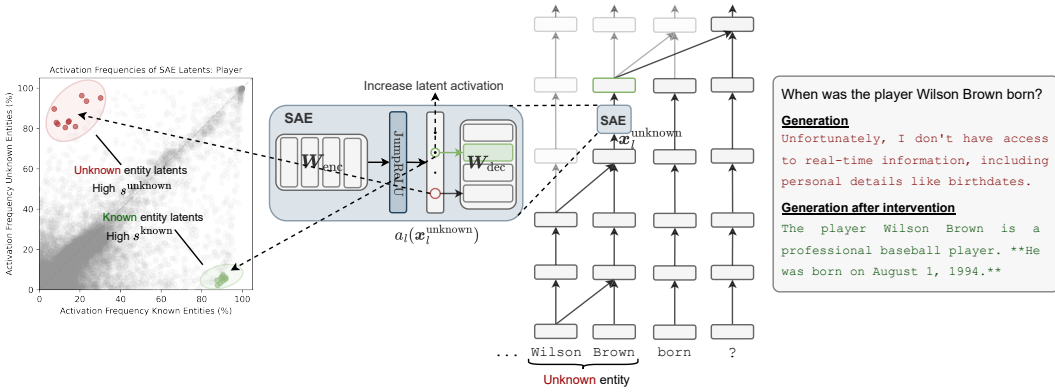


Figure 1: We identify SAE latents in the final token of the entity residual stream (i.e. hidden state) that almost exclusively activate on either unknown or known entities (scatter plot on the left). Modulating the activation values of these latents, e.g. increasing the known entity latent when asking a question about a made-up athlete increases the tendency to hallucinate.

zero below the threshold, and then the identity, with a discontinuous jump at the threshold.  $W_{enc}$ ,  $b_{enc}$  and  $W_{dec}$ ,  $b_{dec}$  are the weight matrices and bias of the encoder and decoder respectively. We refer to *latent activation* to a component in  $a(x)$ , while we reserve the term *latent direction* to a (row) vector in the dictionary  $W_{dec}$ .

Equation (1) shows that the model representation can be approximately reconstructed by a linear combination of the *SAE decoder latents*, which often represent monosemantic features (Cunningham et al., 2023; Bricken et al., 2023; Templeton et al., 2024; Gao et al., 2024). By incorporating a sparsity penalty into the training loss function, we can constrain this reconstruction to be a sparse linear combination, thereby enhancing interpretability:

$$\mathcal{L}(x) = \underbrace{\|x - \text{SAE}(x)\|_2^2}_{\mathcal{L}_{\text{reconstruction}}} + \lambda \underbrace{\|a(x)\|_0}_{\mathcal{L}_{\text{sparsity}}}. \quad (3)$$

**Steering with SAE Latents.** Recall from Equation (1) that SAEs reconstruct a model’s representation as  $x \approx a(x)W_{dec} + b_{dec}$ . This means that the reconstruction is a linear combination of the decoder latents (rows) of  $W_{dec}$  plus a bias, i.e.  $x \approx \sum_j a_j(x)W_{dec}[j, :]$ . Thus, increasing/decreasing the activation value of an SAE latent,  $a_j(x)$ , is equivalent to doing activation steering (Turner et al., 2023) with the decoder latent vector, i.e. updating the residual stream as follows:

$$x^{\text{new}} \leftarrow x + \alpha d_j. \quad (4)$$

### 3 METHODOLOGY

To study how language models reflect knowledge awareness about entities, we build a dataset with four different entity types: (basketball) players, movies, cities, and songs from Wikidata (Vrandečić & Krötzsch, 2024). For each entity, we extract associated attributes available in Wikidata. Then, we create templates of the form (entity type, entity name, relation, attribute) and prompt Gemma 2 2B and 9B models (Team et al., 2024) to predict the attribute given (entity type, relation, entity name), for instance:

$$\begin{array}{c} \text{Entity type} \downarrow \\ \text{The } \text{movie} \text{ 12 Angry Men } \text{ was directed by } \text{---} \\ \text{Entity name} \uparrow \qquad \qquad \qquad \uparrow \text{Attribute} \end{array} \quad (5)$$

We then categorize entities into ‘known’ or ‘unknown’. Known entities are those where the model gets at least two attributes correct, while unknown are where it gets them all wrong, we discard

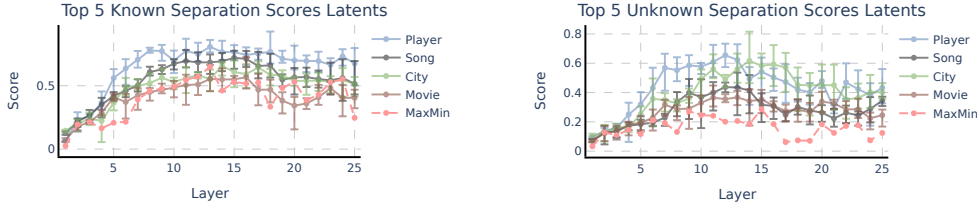


Figure 2: Layerwise evolution of the Top 5 latents in Gemma 2 2B SAEs, as measured by their known (left) and unknown (right) latent separation scores ( $s^{\text{known}}$  and  $s^{\text{unknown}}$ ). Error bars show maximum and minimum scores. MaxMin (red line) refers to the minimum separation score across entities of the best latent. This represents how entity-agnostic is the most general latent per layer. In both cases, the middle layers provide the best-performing latents.

any in-between. To measure correctness we use fuzzy string matching<sup>2</sup>. See Appendix A for a description of the process. We acknowledge that this methodology might introduce some labeling inaccuracies, as the model could ‘guess’ some attributes despite not knowing about the entity or fail to recall the specific attributes we consider while knowing about the entity. However, our primary objective is to achieve a reasonable differentiation between entities rather than striving for perfect classification accuracy. Finally, we split the entities into train/validation/test (50%, 10%, 40%) sets.

We run the model on the set of prompts containing known and unknown entities. Inspired by Meng et al. (2022a); Geva et al. (2023); Nanda et al. (2023) we use the residual stream of the final token of the entity,  $\mathbf{x}^{\text{known}}$  and  $\mathbf{x}^{\text{unknown}}$ . In each layer ( $l$ ), we compute the activations of each latent in the SAE, i.e.  $a_{l,j}(\mathbf{x}_i^{\text{known}})$  and  $a_{l,j}(\mathbf{x}_i^{\text{unknown}})$ . For each latent, we obtain the fraction of the time that it is active (i.e. has a value greater than zero) on known and unknown entities respectively:

$$f_{l,j}^{\text{known}} = \frac{\sum_i^{N^{\text{known}}} \mathbb{1}[a_{l,j}(\mathbf{x}_{l,i}^{\text{known}}) > 0]}{N^{\text{known}}}, \quad f_{l,j}^{\text{unknown}} = \frac{\sum_i^{N^{\text{unknown}}} \mathbb{1}[a_{l,j}(\mathbf{x}_{l,i}^{\text{unknown}}) > 0]}{N^{\text{unknown}}}, \quad (6)$$

where  $N^{\text{known}}$  and  $N^{\text{unknown}}$  are the total number of prompts in each subset. Then, we take the difference, obtaining the *latent separation scores*  $s_{l,j}^{\text{known}} = f_{l,j}^{\text{known}} - f_{l,j}^{\text{unknown}}$  and  $s_{l,j}^{\text{unknown}} = f_{l,j}^{\text{unknown}} - f_{l,j}^{\text{known}}$ , for detecting known and unknown entities respectively.

#### 4 SPARSE AUTOENCODERS UNCOVER ENTITY RECOGNITION DIRECTIONS

We find that the separation scores of some of the SAE latents in the training set are high, i.e. they fire almost exclusively on tokens of either known or unknown entities, as depicted in the scatter plot in Figure 1 for Gemma 2 2B and Figure 8, Appendix C for Gemma 2 9B. An interesting observation is that latent separation scores reveal a consistent pattern across all entity types, with scores increasing throughout the model and reaching a peak around layer 9 before plateauing (Figure 2). This indicates that *latents better distinguishing between known and unknown entities are found in the middle layers*.

We also examine the level of generality of the latents by measuring their minimum separation score across entity types ( $t$ ): players, song, cities and movies. A high minimum separation score indicates that a latent performs robustly across entity types, suggesting strong generalization capabilities. For this purpose, for each layer ( $l$ ) we compute  $\text{MaxMin}^{\text{known},l} = \max_j \min_t s_{l,j}^{\text{known},t}$ , and similarly for unknown entities. The increasing trend shown in the MaxMin (red) line in Figure 2 for Gemma 2 2B and in Figure 9, Appendix D for Gemma 2 9B suggests that more *generalized* latents—those that distinguish between known and unknown entities across various entity types—are concentrated in these intermediate layers. This finding points to a hierarchical organization of entity representation within the model, with more specialized, worse quality, latents in earlier layers and more generalized, higher quality entity-type-agnostic features emerging in the middle layers.

Next, we compute the minimum separation scores by considering every SAE latent in every layer, i.e.  $\min_t s_{l,j}^{\text{known},t}$  for  $1 \leq l \leq L$  and  $1 \leq j \leq d_{\text{SAE}}$ , and equivalently for unknown entities.

<sup>2</sup><https://github.com/seatgeek/thefuzz>.



To ensure specificity to entity tokens, we exclude latents that activate frequently (>2%) on random tokens sampled from the Pile dataset (Gao et al., 2020). The latents with highest minimum separation scores exhibit the most generalized behavior out of all latents, and will be the focus of our subsequent analysis:

$$\text{known entity latent} = \arg \max_{l,j} \min_t \underbrace{s_{l,j}^{\text{known},t}}_{\text{min known separation score of latent } l, j \text{ across entity types}} \text{ and } \text{unknown entity latent} = \arg \max_{l,j} \min_t \underbrace{s_{l,j}^{\text{unknown},t}}_{\text{min unknown separation score of latent } l, j \text{ across entity types}}. \quad (7)$$

Table 1 demonstrates the activation patterns of the Gemma 2 2B topmost known entity latent on prompts with well-known entities (left), and the patterns for the topmost unknown entity latent (right), firing across entities of different types that cannot be recognized. In Appendix B we provide the activations of these latents on sentences containing a diverse set of entity types, suggesting that indeed they are highly general. To validate these latents’ reliability, we analyze their activation frequencies on 283 song titles released after the models’ knowledge cutoff (August 2024). As hypothesized, unknown entity latents show higher activation rates, while known entity latents exhibit lower activation frequencies (Appendix R). While we acknowledge potential overlap between these song titles and pre-training data, the consistent activation patterns across multiple models strengthen our confidence in these latents’ ability to distinguish between known and unknown information. In the following sections, we explore how these primary entity recognition latents influence the model’s overall behavior.

## 5 ENTITY RECOGNITION DIRECTIONS CAUSALLY AFFECT KNOWLEDGE REFUSAL

We define *knowledge refusal* as the model declining to answer a question due to reasons like a lack of information or database access as justification, rather than safety concerns. To quantify knowledge refusals, we adapt the factual recall prompts as in Example 5 into questions:



and we define a set of common knowledge refusal completions and detect if any of these occur with string matching, e.g. ‘Unfortunately, I don’t have access to real-time information...’. Gemma 2 includes both a base model, and a fine-tuned chat (i.e. instruction tuned) model. In Section 4 we found the entity recognition latents by studying the base model, but here focus on the chat model, as they have been explicitly fine-tuned to perform knowledge refusal where appropriate (Team et al., 2024)<sup>3</sup>, and the factuality of chat models is highly desirable.

We hypothesize that entity recognition directions could be used by chat models to induce knowledge refusal. To evaluate this, we use a test set sample of 100 questions about unknown entities, and measure the number of times the model refuses by steering (as in Equation (4)) with the entity recognition latents the last token of the entity and the following end-of-instruction-tokens.<sup>4</sup> Figure 3 (left) illustrates the original model refusal rate (blue bar), showing some refusal across entity types. We see that the entity recognition SAE latents found in the base model transfer to the chat model, and increasing the unknown entity latent induces almost 100% refusal across all entity types in Gemma 2 2B. Conversely, increasing the known entity latent activation slightly reduces refusal rates. We also include an *Orthogonalized model* baseline, which consists of doing weight orthogonalization (Arditi et al., 2024) on every matrix writing to the residual stream. Weight orthogonalization modifies each

<sup>3</sup>The Gemma 2 technical report (Team et al., 2024) mentions “including subsets of data that encourage refusals to minimize hallucinations improves performance on factuality metrics”. This pattern is consistent with recent language models, such as Llama 3.1 (Dubey et al., 2024), where the explicit finetuning process for knowledge refusal has been documented.

<sup>4</sup>We use a validation set to select an appropriate steering coefficient  $\alpha$ . In Appendix G we show generations of Gemma 2B IT with different steering coefficients. We select  $\alpha \in [400, 550]$ , which corresponds to around two times the norm of the residual stream in the layers where the entity recognition latents are present (Appendix E).

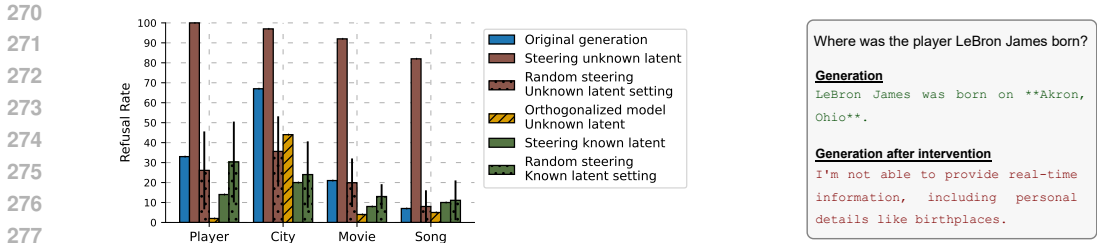


Figure 3: **Left:** Number of times Gemma 2 2B refuses to answer in 100 queries about unknown entities. We examine the unmodified original model, the model steered with the known entity latent and unknown entity latent, and the model with the unknown entity latent projected out of its weights (referred to as Orthogonalized model). The mean and standard deviation of steering with 10 random latents are shown for comparison. **Right:** This example illustrates the effect of steering with the unknown entity recognition latent (same as in Table 1). The steering induces the model to refuse to answer about a well-known basketball player.

row of a weight matrix to make it perpendicular to a specified direction vector  $d$ . This is achieved by subtracting the component of each row that is parallel to  $d$ :

$$W_{out}^{new} \leftarrow W_{out} - W_{out}d^T d. \tag{9}$$

By doing this operation on every output matrix in the model we ensure no component is able to write into that direction. The resulting **orthogonalized model with the top unknown entity direction exhibits a large reduction in refusal responses**, suggesting this direction plays a crucial role in the model’s knowledge refusal behavior. We also include the average refusal rate after steering with 10 different random latents, using the same configuration (layer and steering coefficient) that the known and unknown entity latents respectively. Additional analysis of the Gemma 2 9B model, detailed in Section F, reveals similar patterns, albeit with less pronounced effects compared to the 2B model.

Figure 3 (right) shows a refusal response for a well-known basketball player generated by steering with the unknown entity latent. In Figure 1 (right) we observe that when asked about a non-existent player, Wilson Brown, the model without intervention refuses to answer. However, steering with the known entity latent induces a hallucination.

## 6 MECHANISTIC ANALYSIS

**Entity Recognition Directions Regulate Attention to Entity.** In the previous section, we saw that entity recognition latents had a causal effect on knowledge refusal. Here, we look at how they affect the factual recall mechanism (*aka* circuit) in prompts of the format of Example 5. This has been well studied before on other language models (Nanda et al., 2023; Geva et al., 2023; Meng et al., 2022a). We replicate the approach of Nanda et al. (2023) on Gemma 2 2B and 9B and find a similar circuit. Namely, early attention heads merge the entity’s name into the last token of the entity, and downstream attention heads extract relevant attributes from the entity and move them to the final token position (Figure 4 (a, b)), this pattern holds across various entity types and model sizes (Appendix I and Appendix J). To do the analysis, we perform activation patching (Geiger et al., 2020; Vig et al., 2020; Meng et al., 2022a) on the residual streams and attention heads’ outputs (see Appendix H for a detailed explanation on the method). We use the denoising setup (Heimersheim & Nanda, 2024), where we patch representations from a clean run (with a known entity) and apply it over the run with a corrupted input (with an unknown entity).<sup>5</sup>

Expanding on the findings of Yuksekgonul et al. (2024), who established a link between prediction accuracy and attention to the entity tokens, our study reveals a large disparity in attention between known and unknown entities, for instance the attribute extraction heads L18H5 and L20H3 (Figure 4 (c)), which are overall relevant across entity types in Gemma 2 2B (see example of attributes

<sup>5</sup>We show the proportion of logit difference recovered after each patch in Figure 4 (a). A recovered logit difference of 1 indicates that the prediction after patching is the same as the original prediction in the clean run.

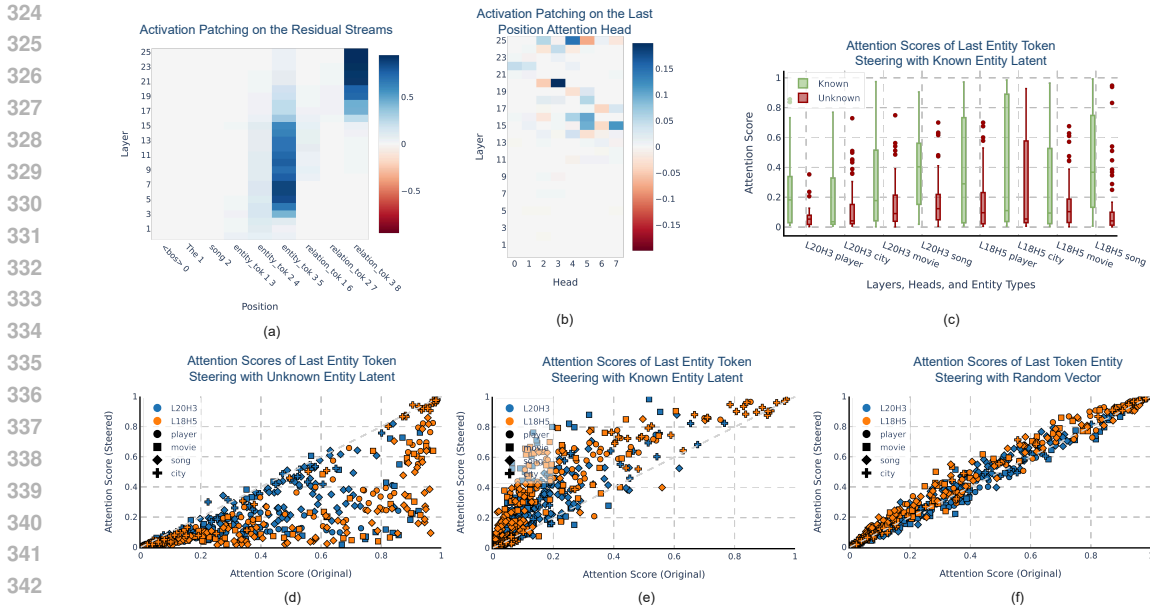


Figure 4: (a,b) Activation patching on the residual streams and the output of attention heads in the last position (song entities). We patch clean (from known entities prompts) representations into a corrupted forward pass (from unknown entities prompts) and measure the logit difference recovered. (c) Attention paid from the last position to the last token of the entity is greater when faced with a known entity in attribute-extraction heads. (d,e,f) Effect on attention scores, as in (c), after steering the last token of the entity with the unknown entity latent (d), known entity latent (e), and a random vector with same norm (f).

extracted by these heads in Appendix L). Notably, attention scores are higher when faced with a known entity. This suggests that the detected entity recognition latents might influence the attention mechanism through the ‘keys’ computation to induce this behavior. To evaluate this hypothesis we steer the residual stream with the found latents on the last token of the entity, and measure the attention scores of the entity tokens. We observe a causal relationship between the entity recognition latents and the attention patterns of the attention heads downstream, being more pronounced in the attribute extraction heads. Steering with the top unknown entity latent reduces the attention to entity, even in prompts with a known entity (Figure 4 (d)), while steering with the known entity latent increases the attention scores (Figure 4 (e)). We show in Figure 4 (f) the results of steering with a random unit vector baseline for comparison, and in Appendix K when steering with a random SAE latent. In Appendix L we illustrate the average attention score change to the entity tokens after steering on the residual streams of the last token of the entities in Gemma 2 2B and 9B with the top 3 known and unknown entity latents. The results reveal an increase/decrease attention score across upper layer heads, with the 9B model showing more subtle effects when steered using unknown latents.

These results provide compelling evidence that the entity recognition SAE latent directions play a crucial role in regulating the model’s attention mechanisms, and thereby their ability to extract attributes.

**Early Entity Recognition Directions Regulate Expressing Knowledge Uncertainty.** We have shown that the entity recognition latents causally affect the model’s knowledge refusal, implicitly using its knowledge of whether it recognises an entity, but not whether they are used when explicitly asking a model whether it recognises an entity. To investigate this, we use the following prompt structure:

Are you sure you know the {entity\_type} {entity}? Answer yes or no. Answer: \_\_\_\_\_ (10)

378  
379  
380  
381  
382  
383  
384  
385  
386  
387  
388  
389  
390  
391  
392  
393  
394  
395  
396  
397  
398  
399  
400  
401  
402  
403  
404  
405  
406  
407  
408  
409  
410  
411  
412  
413  
414  
415  
416  
417  
418  
419  
420  
421  
422  
423  
424  
425  
426  
427  
428  
429  
430  
431

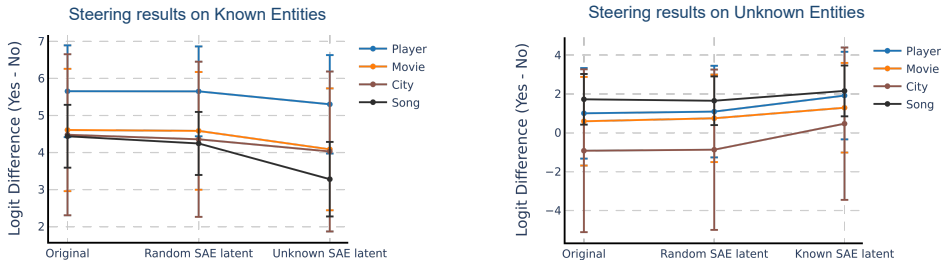


Figure 5: Logit difference between “Yes” and “No” predictions on the question “Are you sure you know the {entity\_type} {entity\_name}? Answer yes or no.” after steering with unknown (left) and known (right) entity recognition latents.

We then steer the residual streams of the last token of the entity by upweighting the entity recognition latents. In Figure 5 we show the results on the logit difference between Yes and No responses. The left plot illustrates the effect of steering known entities prompts with the unknown entity latent. This intervention results in a reduction of the logit difference. For comparison, we include a random baseline where we apply a randomly sampled SAE latent with the same coefficient. In the right plot, we steer unknown entities prompts with the known entity latent. Despite the model’s inherent bias towards Yes predictions for unknown entities (indicated by positive logit differences in the ‘Original’ column), which indicates the model struggles to accurately express their uncertainty (Yona et al., 2024), this intervention leads to a positive shift in the logit difference, suggesting that the entity recognition latents, although slightly, have an effect on the expression of uncertainty about knowledge of entities. A similar pattern can be observed in Gemma 2 9B (Appendix N).

## 7 UNCERTAINTY DIRECTIONS

Having studied how base models represent features for entity recognition, we now explore internal representations that may differentiate between correct and wrong answers. Our investigation focuses on chat models, which are capable of refusing to answer, and we search for directions in the representation space signaling uncertainty or lack of knowledge potentially indicative of upcoming errors. For this analysis we use our entities dataset, and exclude instances where the model refuses to respond, and leave only prompts that elicit either correct predictions or errors from the model.

Our study focuses on the study of the residual streams *before* the answer. We hypothesize that end-of-instruction tokens, which always succeed the instruction, may aggregate information about the whole question (Marks & Tegmark, 2023).<sup>6</sup> We select the token model and use examples such as:

<start\_of\_turn>user\nWhen was the player Wilson Brown born?<end\_of\_turn>\n<start\_of\_turn>model\n (11)

For each entity type and layer with available SAE we extract the representations of the model residual stream, for both correct and mistaken answers, and gather the SAE latent activations. We are interested in seeing whether there are SAE latents that convey information about how unsure or uncertain the model is to answer to a question, but still fails to refuse, giving rise to hallucinations. We divide the dataset of prompts into train/validation/test sets (50%, 10%, 40%).

To capture subtle variations in model uncertainty, which may be represented even when attributes are correctly recalled, we focus on quantifying differences in activation levels between correct and incorrect responses. For each latent, we compute the t-statistic in the training set using two activation samples:  $a_{l,j}(\mathbf{x}_l^{\text{correct}})$  for correct responses and  $a_{l,j}(\mathbf{x}_l^{\text{error}})$  for incorrect ones. The t-statistic measures how different the two sample means are from each other, taking into account the variability within the samples:

$$t\text{-statistic}_{l,j} = \frac{\mu(a_{l,j}(\mathbf{x}_l^{\text{correct}})) - \mu(a_{l,j}(\mathbf{x}_l^{\text{error}}))}{\sqrt{\frac{\sigma(a_{l,j}(\mathbf{x}_l^{\text{correct}}))^2}{n_{\text{correct}}} + \frac{\sigma(a_{l,j}(\mathbf{x}_l^{\text{error}}))^2}{n_{\text{error}}}}}. \tag{12}$$

<sup>6</sup>This concept was termed by Tigges et al. (2023) as the ‘summarization motif’.

432  
433  
434  
435  
436  
437  
438  
439

‘Unknown’ Latent Activations
“Apparently one or two people were shooting or shooting at each other for reasons unknown when eight people were struck by the gunfire
...and the Red Cross all responded to the fire. The cause of the fire remains under investigation.
The Witcher Card Game will have another round of beta tests this spring (platforms TBA)
His condition was not disclosed, but police said he was described as stable.

440  
441  
442

Table 2: Activations of the Gemma 2B IT ‘unknown’ latent on the maximally activating examples provided by Neuropedia (Lin & Bloom, 2024).

443  
444  
445  
446  
447  
448  
449  
450  
451  
452  
453  
454  
455  
456

We use a pre-trained SAE for the 13th layer (out of 18) of Gemma 2B IT<sup>7</sup>, and the available Gemma Scope SAEs for Gemma 2 9B IT, at layers 10, 21, and 32 (out of 42). Our approach for detecting top latents, similar to the entity recognition method described in Section 4 focuses on the top latents with the highest minimum t-statistic score across entities, representing the most general latents. We split the dataset into train and test sets, and use the training set to select the top latents. The left panel of Figure 6 reveals a distinct separation between the latent activations at the model token when comparing correct versus incorrect responses in the test set. Using this latent as a classifier, it achieves 73.2 AUROC score, and by calibrating the decision threshold on a validation set, it gets an F1 score of 72. See Appendix P with separated errors by entity type. Table 2 illustrates the activations of the highest-scoring latent in Gemma 2B IT’s SAE on a large text corpus (Penedo et al., 2024)<sup>8</sup>, showing it triggers on text related to uncertainty or undisclosed information. Figure 6 (right) illustrates the top tokens with higher logit increase by this latent, further confirming its association with concepts of unknownness.<sup>9</sup> Similar latent separations between correct and incorrect answers can also be observed in Gemma 2 9B IT (Appendix O).

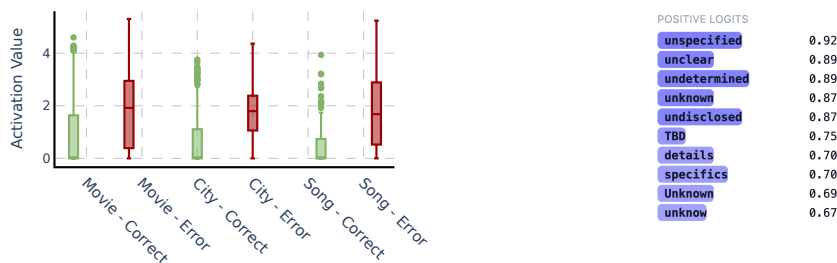
457  
458  
459  
460  
461  
462  
463  
464  
465466  
467

Figure 6: **Left:** Activation values of the Gemma 2B IT ‘unknown’ latent on correct and incorrect responses. **Right:** Top 10 tokens with the highest logit increase by the ‘unknown’ latent influence.

468  
469

## 8 RELATED WORK

470  
471  
472  
473  
474  
475  
476  
477  
478  
479  
480  
481  
482

Recent advances in mechanistic interpretability in language models (Ferrando et al., 2024) have shed light on the factual recall process in these systems. Key discoveries include the aggregation of entity tokens (Nanda et al., 2023), the importance of early MLPs for entity processing (Meng et al., 2022b), and the identification of specialized extraction relation heads (Geva et al., 2023; Chughtai et al., 2024). Despite these insights, there remains a significant gap in our understanding of the mechanisms underlying failures in attribute extraction leading to hallucinations. Gottesman & Geva (2024) demonstrated that the performance of probes trained on the residual streams of entities correlates with the model’s ability to answer questions about them accurately. Yuksekogonul et al. (2024) established a link between increased attention to entity tokens and improved factual accuracy. (Yu et al., 2024) proposed two mechanisms for non-factual hallucinations: inadequate entity enrichment in early MLPs and failure to extract correct attributes in upper layers. Our research aligns with

483  
484  
485

<sup>7</sup><https://huggingface.co/jbloom/Gemma-2b-IT-Residual-Stream-SAEs>. We note that Gemma Scope doesn’t provide SAEs for Gemma 2 2B IT.

<sup>8</sup><https://huggingface.co/datasets/HuggingFaceFW/fineweb>.

<sup>9</sup>We omit the players category since Gemma 2B IT refuses to almost all of those queries.



486 studies on hallucination prediction (Kossen et al., 2024; Varshney et al., 2023), particularly those  
 487 engaging with model internals (CH-Wang et al., 2023; Azaria & Mitchell, 2023). Previous work  
 488 has trained probes to predict truthfulness of the produced outputs (Li et al., 2023) with Joshi et al.  
 489 (2024) showing this can be detected in activation space before the model generation, which can be  
 490 related to our results on ‘uncertainty directions’ discovered in Section 7. Additionally, our work  
 491 contributes to the growing body of literature on practical applications of sparse autoencoders, as  
 492 investigated by Marks et al. (2024); Krzyzanowski et al. (2024). While the practical applications  
 493 of sparse autoencoders in language model interpretation are still in their early stages, our research  
 494 demonstrates their potential.

## 495 9 CONCLUSIONS

496 In this paper, we use sparse autoencoders to identify directions in the model’s representation space  
 497 that suggest the presence of encoded knowledge awareness about entities. These directions,  
 498 found in the base model, are causally relevant to the knowledge refusal behavior in the chat-based  
 499 model. We demonstrated that, by manipulating these directions, we can control the model’s tendency  
 500 to refuse answers or hallucinate information. We also provide insights into how the entity recogni-  
 501 tion directions influence the model behavior, such as regulating the attention paid to entity tokens,  
 502 and their influence in expressing knowledge uncertainty. Finally, we uncover directions representing  
 503 model uncertainty to specific queries, capable of discriminating between correct and mistaken an-  
 504 swers. While our primary focus in this work centers on the representation of knowledge awareness  
 505 and uncertainty, the methodology we present for discovering these latent directions is generalizable  
 506 to any other type of binary (Section 3) and continuous (Section 7) features. This work contributes to  
 507 our understanding of language model behavior and opens avenues for improving model reliability  
 508 and mitigating hallucinations.

## 509 REFERENCES

- 510 Andy Ardit, Oscar Obeso, Aaquib Syed, Daniel Paleka, Nina Panickssery, Wes Gurnee, and Neel  
 511 Nanda. Refusal in language models is mediated by a single direction. *ArXiv*, 2024. URL <https://arxiv.org/abs/2406.11717>.
- 512 Amos Azaria and Tom Mitchell. The internal state of an LLM knows when it’s lying. In Houda  
 513 Bouamor, Juan Pino, and Kalika Bali (eds.), *Findings of the Association for Computational Lin-*  
 514 *guistics: EMNLP 2023*, pp. 967–976, Singapore, December 2023. Association for Computa-  
 515 tional Linguistics. doi: 10.18653/v1/2023.findings-emnlp.68. URL <https://aclanthology.org/2023.findings-emnlp.68>.
- 516 Trenton Bricken, Adly Templeton, Joshua Batson, Brian Chen, Adam Jermyn, Tom Conerly, Nick  
 517 Turner, Cem Anil, Carson Denison, Amanda Askell, Robert Lasenby, Yifan Wu, Shauna Kravec,  
 518 Nicholas Schiefer, Tim Maxwell, Nicholas Joseph, Zac Hatfield-Dodds, Alex Tamkin, Karina  
 519 Nguyen, Brayden McLean, Josiah E Burke, Tristan Hume, Shan Carter, Tom Henighan, and  
 520 Christopher Olah. Towards monosemanticity: Decomposing language models with dictionary  
 521 learning. *Transformer Circuits Thread*, 2023. URL <https://transformer-circuits.pub/2023/monosemantic-features/index.html>.
- 522 Tom Brown, Benjamin Mann, Nick Ryder, Melanie Subbiah, Jared D Kaplan, Prafulla Dhari-  
 523 wal, Arvind Neelakantan, Pranav Shyam, Girish Sastry, Amanda Askell, Sandhini Agar-  
 524 wal, Ariel Herbert-Voss, Gretchen Krueger, Tom Henighan, Rewon Child, Aditya Ramesh,  
 525 Daniel Ziegler, Jeffrey Wu, Clemens Winter, Chris Hesse, Mark Chen, Eric Sigler, Ma-  
 526 teusz Litwin, Scott Gray, Benjamin Chess, Jack Clark, Christopher Berner, Sam McCand-  
 527 lish, Alec Radford, Ilya Sutskever, and Dario Amodei. Language models are few-shot  
 528 learners. In H. Larochelle, M. Ranzato, R. Hadsell, M.F. Balcan, and H. Lin (eds.), *Ad-*  
 529 *vances in Neural Information Processing Systems*, volume 33, pp. 1877–1901. Curran As-  
 530 sociates, Inc., 2020. URL [https://proceedings.neurips.cc/paper\\_files/paper/2020/](https://proceedings.neurips.cc/paper_files/paper/2020/file/1457c0d6bfc4967418bfb8ac142f64a-Paper.pdf)  
 531 [file/1457c0d6bfc4967418bfb8ac142f64a-Paper.pdf](https://proceedings.neurips.cc/paper_files/paper/2020/file/1457c0d6bfc4967418bfb8ac142f64a-Paper.pdf).
- 532 Sky CH-Wang, Benjamin Van Durme, Jason Eisner, and Chris Kedzie. Do androids know they’re  
 533 only dreaming of electric sheep?, 2023. URL <https://arxiv.org/abs/2312.17249v1>.

- 540 Aakanksha Chowdhery, Sharan Narang, Jacob Devlin, Maarten Bosma, Gaurav Mishra, Adam  
541 Roberts, Paul Barham, Hyung Won Chung, Charles Sutton, Sebastian Gehrmann, Parker Schuh,  
542 Kensen Shi, Sasha Tsvyashchenko, Joshua Maynez, Abhishek Rao, Parker Barnes, Yi Tay, Noam  
543 Shazeer, Vinodkumar Prabhakaran, Emily Reif, Nan Du, Ben Hutchinson, Reiner Pope, James  
544 Bradbury, Jacob Austin, Michael Isard, Guy Gur-Ari, Pengcheng Yin, Toju Duke, Anselm Lev-  
545 skaya, Sanjay Ghemawat, Sunipa Dev, Henryk Michalewski, Xavier Garcia, Vedant Misra, Kevin  
546 Robinson, Liam Fedus, Denny Zhou, Daphne Ippolito, David Luan, Hyeontaek Lim, Barret  
547 Zoph, Alexander Spiridonov, Ryan Sepassi, David Dohan, Shivani Agrawal, Mark Omernick,  
548 Andrew M. Dai, Thanumalayan Sankaranarayana Pillai, Marie Pellat, Aitor Lewkowycz, Er-  
549 ica Moreira, Rewon Child, Oleksandr Polozov, Katherine Lee, Zongwei Zhou, Xuezhi Wang,  
550 Brennan Saeta, Mark Diaz, Orhan Firat, Michele Catasta, Jason Wei, Kathy Meier-Hellstern,  
551 Douglas Eck, Jeff Dean, Slav Petrov, and Noah Fiedel. Palm: Scaling language modeling  
552 with pathways. *Journal of Machine Learning Research*, 24(240):1–113, 2023. URL [http:  
553 //jmlr.org/papers/v24/22-1144.html](http://jmlr.org/papers/v24/22-1144.html).
- 554 Bilal Chughtai, Alan Cooney, and Neel Nanda. Summing up the facts: Additive mechanisms behind  
555 factual recall in llms, 2024. URL <https://www.arxiv.org/abs/2402.07321>.
- 556 Hoagy Cunningham, Aidan Ewart, Logan Riggs, Robert Huben, and Lee Sharkey. Sparse au-  
557 toencoders find highly interpretable features in language models. *Arxiv*, 2023. URL [https:  
558 //arxiv.org/abs/2309.08600](https://arxiv.org/abs/2309.08600).
- 559 Abhimanyu Dubey, Abhinav Jauhri, Abhinav Pandey, Abhishek Kadian, Ahmad Al-Dahle, Aiesha  
560 Letman, Akhil Mathur, Alan Schelten, Amy Yang, Angela Fan, Anirudh Goyal, Anthony  
561 Hartshorn, Aobo Yang, Archi Mitra, Archie Sravankumar, Artem Korenev, Arthur Hinsvark,  
562 Arun Rao, Aston Zhang, Aurelien Rodriguez, Austen Gregerson, Ava Spataru, Baptiste Roziere,  
563 Bethany Biron, Binh Tang, Bobbie Chern, Charlotte Caucheteux, Chaya Nayak, Chloe Bi, Chris  
564 Marra, Chris McConnell, Christian Keller, Christophe Touret, Chunyang Wu, Corinne Wong,  
565 Cristian Canton Ferrer, Cyrus Nikolaidis, Damien Allonsius, Daniel Song, Danielle Pintz, Danny  
566 Livshits, David Esiobu, Dhruv Choudhary, Dhruv Mahajan, Diego Garcia-Olano, Diego Perino,  
567 Dieuwke Hupkes, Egor Lakomkin, Ehab AlBadawy, Elina Lobanova, Emily Dinan, Eric Michael  
568 Smith, Filip Radenovic, Frank Zhang, Gabriel Synnaeve, Gabrielle Lee, Georgia Lewis Ander-  
569 son, Graeme Nail, Gregoire Mialon, Guan Pang, Guillem Cucurell, Hailey Nguyen, Hannah  
570 Korevaar, Hu Xu, Hugo Touvron, Iliyan Zarov, Imanol Arrieta Ibarra, Isabel Kloumann, Ishan  
571 Misra, Ivan Evtimov, Jade Copet, Jaewon Lee, Jan Geffert, Jana Vranes, Jason Park, Jay Ma-  
572 hadeokar, Jeet Shah, Jelmer van der Linde, Jennifer Billock, Jenny Hong, Jenya Lee, Jeremy  
573 Fu, Jianfeng Chi, Jianyu Huang, Jiawen Liu, Jie Wang, Jiecao Yu, Joanna Bitton, Joe Spisak,  
574 Jongsoo Park, Joseph Rocca, Joshua Johnstun, Joshua Saxe, Junteng Jia, Kalyan Vasuden Al-  
575 wala, Kartikeya Upasani, Kate Plawiak, Ke Li, Kenneth Heafield, Kevin Stone, Khalid El-Arini,  
576 Krithika Iyer, Kshitiz Malik, Kuenley Chiu, Kunal Bhalla, Lauren Rantala-Yearly, Laurens van der  
577 Maaten, Lawrence Chen, Liang Tan, Liz Jenkins, Louis Martin, Lovish Madaan, Lubo Malo,  
578 Lukas Blecher, Lukas Landzaat, Luke de Oliveira, Madeline Muzzi, Mahesh Pasupuleti, Man-  
579 nat Singh, Manohar Paluri, Marcin Kardas, Mathew Oldham, Mathieu Rita, Maya Pavlova,  
580 Melanie Kambadur, Mike Lewis, Min Si, Mitesh Kumar Singh, Mona Hassan, Naman Goyal,  
581 Narjes Torabi, Nikolay Bashlykov, Nikolay Bogoychev, Niladri Chatterji, Olivier Duchenne, Onur  
582 Çelebi, Patrick Alrassy, Pengchuan Zhang, Pengwei Li, Petar Vasic, Peter Weng, Prajwal Bhar-  
583 gava, Pratik Dubal, Praveen Krishnan, Punit Singh Koura, Puxin Xu, Qing He, Qingxiao Dong,  
584 Ragavan Srinivasan, Raj Ganapathy, Ramon Calderer, Ricardo Silveira Cabral, Robert Stojnic,  
585 Roberta Raileanu, Rohit Girdhar, Rohit Patel, Romain Sauvestre, Ronnie Polidoro, Roshan Sum-  
586 baly, Ross Taylor, Ruan Silva, Rui Hou, Rui Wang, Saghar Hosseini, Sahana Chennabasappa,  
587 Sanjay Singh, Sean Bell, Seohyun Sonia Kim, Sergey Edunov, Shaoliang Nie, Sharan Narang,  
588 Sharath Rapparthi, Sheng Shen, Shengye Wan, Shruti Bhosale, Shun Zhang, Simon Vandenhende,  
589 Soumya Batra, Spencer Whitman, Sten Sootla, Stephane Collot, Suchin Gururangan, Sydney  
590 Borodinsky, Tamar Herman, Tara Fowler, Tarek Sheasha, Thomas Georgiou, Thomas Scialom,  
591 Tobias Speckbacher, Todor Mihaylov, Tong Xiao, Ujjwal Karn, Vedanuj Goswami, Vibhor Gupta,  
592 Vignesh Ramanathan, Viktor Kerkez, Vincent Gonguet, Virginie Do, Vish Vogeti, Vladan Petro-  
593 vic, Weiwei Chu, Wenhan Xiong, Wenyin Fu, Whitney Meers, Xavier Martinet, Xiaodong Wang,  
Xiaoqing Ellen Tan, Xinfeng Xie, Xuchao Jia, Xuwei Wang, Yaelle Goldschlag, Yashesh Gaur,  
Yasmine Babaei, Yi Wen, Yiwen Song, Yuchen Zhang, Yue Li, Yuning Mao, Zacharie Delpierre  
Coudert, Zheng Yan, Zhengxing Chen, Zoe Papakipos, Aaditya Singh, Aaron Grattafiori, Abha

- 594 Jain, Adam Kelsey, Adam Shajnfeld, Adithya Gangidi, Adolfo Victoria, Ahuva Goldstand, Ajay  
595 Menon, Ajay Sharma, Alex Boesenberg, Alex Vaughan, Alexei Baevski, Allie Feinstein, Amanda  
596 Kallet, Amit Sangani, Anam Yunus, Andrei Lupu, Andres Alvarado, Andrew Caples, Andrew  
597 Gu, Andrew Ho, Andrew Poulton, Andrew Ryan, Ankit Ramchandani, Annie Franco, Aparajita  
598 Saraf, Arkabandhu Chowdhury, Ashley Gabriel, Ashwin Bharambe, Assaf Eisenman, Azadeh  
599 Yazdan, Beau James, Ben Maurer, Benjamin Leonhardi, Bernie Huang, Beth Loyd, Beto De  
600 Paola, Bhargavi Paranjape, Bing Liu, Bo Wu, Boyu Ni, Braden Hancock, Bram Wasti, Bran-  
601 don Spence, Brani Stojkovic, Brian Gamido, Britt Montalvo, Carl Parker, Carly Burton, Catalina  
602 Mejia, Changhan Wang, Changkyu Kim, Chao Zhou, Chester Hu, Ching-Hsiang Chu, Chris Cai,  
603 Chris Tindal, Christoph Feichtenhofer, Damon Civin, Dana Beaty, Daniel Kreymer, Daniel Li,  
604 Danny Wyatt, David Adkins, David Xu, Davide Testuggine, Delia David, Devi Parikh, Diana  
605 Liskovich, Didem Foss, Ding Kang Wang, Duc Le, Dustin Holland, Edward Dowling, Eissa Jamil,  
606 Elaine Montgomery, Eleonora Presani, Emily Hahn, Emily Wood, Erik Brinkman, Esteban Ar-  
607 caute, Evan Dunbar, Evan Smothers, Fei Sun, Felix Kreuk, Feng Tian, Firat Ozgenel, Francesco  
608 Caggioni, Francisco Guzmán, Frank Kanayet, Frank Seide, Gabriela Medina Florez, Gabriella  
609 Schwarz, Gada Badeer, Georgia Swee, Gil Halpern, Govind Thattai, Grant Herman, Grigory  
610 Sizov, Guangyi, Zhang, Guna Lakshminarayanan, Hamid Shojanazeri, Han Zou, Hannah Wang,  
611 Hanwen Zha, Haroun Habeeb, Harrison Rudolph, Helen Suk, Henry Aspegren, Hunter Gold-  
612 man, Ibrahim Damla, Igor Molybog, Igor Tufanov, Irina-Elena Veliche, Itai Gat, Jake Weissman,  
613 James Geboski, James Kohli, Japhet Asher, Jean-Baptiste Gaya, Jeff Marcus, Jeff Tang, Jennifer  
614 Chan, Jenny Zhen, Jeremy Reizenstein, Jeremy Teboul, Jessica Zhong, Jian Jin, Jingyi Yang, Joe  
615 Cummings, Jon Carvill, Jon Shepard, Jonathan McPhie, Jonathan Torres, Josh Ginsburg, Junjie  
616 Wang, Kai Wu, Kam Hou U, Karan Saxena, Karthik Prasad, Kartikay Khandelwal, Katayoun  
617 Zand, Kathy Matosich, Kaushik Veeraraghavan, Kelly Michelena, Keqian Li, Kun Huang, Kunal  
618 Chawla, Kushal Lakhota, Kyle Huang, Lailin Chen, Lakshya Garg, Lavender A, Leandro Silva,  
619 Lee Bell, Lei Zhang, Liangpeng Guo, Licheng Yu, Liron Moshkovich, Luca Wehrstedt, Madian  
620 Khabsa, Manav Avalani, Manish Bhatt, Maria Tsimpoukelli, Martynas Mankus, Matan Hasson,  
621 Matthew Lennie, Matthias Reso, Maxim Groshev, Maxim Naumov, Maya Lathi, Meghan Ke-  
622 neally, Michael L. Seltzer, Michal Valko, Michelle Restrepo, Mihir Patel, Mik Vyatskov, Mikayel  
623 Samvelyan, Mike Clark, Mike Macey, Mike Wang, Miquel Jubert Hermoso, Mo Metanat, Mo-  
624 hammad Rastegari, Munish Bansal, Nandhini Santhanam, Natascha Parks, Natasha White, Navy-  
625 ata Bawa, Nayan Singhal, Nick Egebo, Nicolas Usunier, Nikolay Pavlovich Laptev, Ning Dong,  
626 Ning Zhang, Norman Cheng, Oleg Chernoguz, Olivia Hart, Omkar Salpekar, Ozlem Kalinli,  
627 Parkin Kent, Parth Parekh, Paul Saab, Pavan Balaji, Pedro Rittner, Philip Bontrager, Pierre Roux,  
628 Piotr Dollar, Polina Zvyagina, Prashant Ratanchandani, Pritish Yuvraj, Qian Liang, Rachad Alao,  
629 Rachel Rodriguez, Rafi Ayub, Raghotham Murthy, Raghu Nayani, Rahul Mitra, Raymond Li,  
630 Rebekkah Hogan, Robin Battey, Rocky Wang, Rohan Maheswari, Russ Howes, Ruty Rinott,  
631 Sai Jayesh Bondu, Samyak Datta, Sara Chugh, Sara Hunt, Sargun Dhillon, Sasha Sidorov, Sa-  
632 tadru Pan, Saurabh Verma, Seiji Yamamoto, Sharadh Ramaswamy, Shaun Lindsay, Shaun Lind-  
633 say, Sheng Feng, Shenghao Lin, Shengxin Cindy Zha, Shiva Shankar, Shuqiang Zhang, Shuqiang  
634 Zhang, Sinong Wang, Sneha Agarwal, Soji Sajuyigbe, Soumith Chintala, Stephanie Max, Stephen  
635 Chen, Steve Kehoe, Steve Satterfield, Sudarshan Govindaprasad, Sumit Gupta, Sungmin Cho,  
636 Sunny Virk, Suraj Subramanian, Sy Choudhury, Sydney Goldman, Tal Remez, Tamar Glaser,  
637 Tamara Best, Thilo Kohler, Thomas Robinson, Tianhe Li, Tianjun Zhang, Tim Matthews, Tim-  
638 othy Chou, Tzook Shaked, Varun Vontimitta, Victoria Ajayi, Victoria Montanez, Vijai Mohan,  
639 Vinay Satish Kumar, Vishal Mangla, Vitor Albiero, Vlad Ionescu, Vlad Poenaru, Vlad Tiberiu  
640 Mihailescu, Vladimir Ivanov, Wei Li, Wenchen Wang, Wenwen Jiang, Wes Bouaziz, Will Con-  
641 stable, Xiaocheng Tang, Xiaofang Wang, Xiaoqian Wu, Xiaolan Wang, Xide Xia, Xilun Wu,  
642 Xinbo Gao, Yanjun Chen, Ye Hu, Ye Jia, Ye Qi, Yenda Li, Yilin Zhang, Ying Zhang, Yossi Adi,  
643 Youngjin Nam, Yu, Wang, Yuchen Hao, Yundi Qian, Yuzi He, Zach Rait, Zachary DeVito, Zef  
644 Rosnbrick, Zhaoduo Wen, Zhenyu Yang, and Zhiwei Zhao. The llama 3 herd of models. *ArXiv*,  
645 2024. URL <https://arxiv.org/abs/2407.21783>.
- 643 N. Benjamin Erichson, Zhewei Yao, and Michael W. Mahoney. Jumprelu: A retrofit defense strategy  
644 for adversarial attacks. *ArXiv*, 2019. URL <https://arxiv.org/abs/1904.03750>.
- 645  
646 Javier Ferrando, Gabriele Sarti, Arianna Bisazza, and Marta R. Costa-jussà. A primer on the inner  
647 workings of transformer-based language models. *ArXiv*, 2024. URL <https://arxiv.org/abs/2405.00208>.

- 648 Leo Gao, Stella Biderman, Sid Black, Laurence Golding, Travis Hoppe, Charles Foster, Jason  
649 Phang, Horace He, Anish Thite, Noa Nabeshima, Shawn Presser, and Connor Leahy. The Pile:  
650 An 800gb dataset of diverse text for language modeling. *arXiv preprint arXiv:2101.00027*, 2020.  
651
- 652 Leo Gao, Tom Dupré la Tour, Henk Tillman, Gabriel Goh, Rajan Troll, Alec Radford, Ilya Sutskever,  
653 Jan Leike, and Jeffrey Wu. Scaling and evaluating sparse autoencoders. *ArXiv*, 2024. URL  
654 <https://arxiv.org/abs/2406.04093>.
- 655 Atticus Geiger, Kyle Richardson, and Christopher Potts. Neural natural language inference models  
656 partially embed theories of lexical entailment and negation. In Afra Alishahi, Yonatan Belinkov,  
657 Grzegorz Chrupała, Dieuwke Hupkes, Yuval Pinter, and Hassan Sajjad (eds.), *Proceedings of*  
658 *the Third BlackboxNLP Workshop on Analyzing and Interpreting Neural Networks for NLP*, pp.  
659 163–173, Online, November 2020. Association for Computational Linguistics. doi: 10.18653/v1/  
660 2020.blackboxnlp-1.16. URL <https://aclanthology.org/2020.blackboxnlp-1.16>.
- 661  
662 Mor Geva, Jasmijn Bastings, Katja Filippova, and Amir Globerson. Dissecting recall of factual  
663 associations in auto-regressive language models. In Houda Bouamor, Juan Pino, and Kalika  
664 Bali (eds.), *Proceedings of the 2023 Conference on Empirical Methods in Natural Language*  
665 *Processing*, pp. 12216–12235, Singapore, December 2023. Association for Computational Lin-  
666 guistics. doi: 10.18653/v1/2023.emnlp-main.751. URL <https://aclanthology.org/2023.emnlp-main.751>.
- 667  
668 Daniela Gottesman and Mor Geva. Estimating knowledge in large language models without gener-  
669 ating a single token. *ArXiv*, 2024. URL <https://arxiv.org/abs/2406.12673>.
- 670  
671 Aaron Grattafiori, Abhimanyu Dubey, Abhinav Jauhri, Abhinav Pandey, Abhishek Kadian, Ahmad  
672 Al-Dahle, Aiesha Letman, Akhil Mathur, Alan Schelten, Alex Vaughan, Amy Yang, Angela Fan,  
673 Anirudh Goyal, Anthony Hartshorn, Aobo Yang, Archi Mitra, Archie Sravankumar, Artem Ko-  
674 renev, Arthur Hinsvark, Arun Rao, Aston Zhang, Aurelien Rodriguez, Austen Gregerson, Ava  
675 Spataru, Baptiste Roziere, Bethany Biron, Binh Tang, Bobbie Chern, Charlotte Caucheteux,  
676 Chaya Nayak, Chloe Bi, Chris Marra, Chris McConnell, Christian Keller, Christophe Touret,  
677 Chunyang Wu, Corinne Wong, Cristian Canton Ferrer, Cyrus Nikolaidis, Damien Allonsius,  
678 Daniel Song, Danielle Pintz, Danny Livshits, Danny Wyatt, David Esiobu, Dhruv Choudhary,  
679 Dhruv Mahajan, Diego Garcia-Olano, Diego Perino, Dieuwke Hupkes, Egor Lakomkin, Ehab  
680 AlBadawy, Elina Lobanova, Emily Dinan, Eric Michael Smith, Filip Radenovic, Francisco  
681 Guzmán, Frank Zhang, Gabriel Synnaeve, Gabrielle Lee, Georgia Lewis Anderson, Govind That-  
682 tai, Graeme Nail, Gregoire Mialon, Guan Pang, Guillem Cucurell, Hailey Nguyen, Hannah Kore-  
683 vaar, Hu Xu, Hugo Touvron, Iliyan Zarov, Imanol Arrieta Ibarra, Isabel Kloumann, Ishan Misra,  
684 Ivan Evtimov, Jack Zhang, Jade Copet, Jaewon Lee, Jan Geffert, Jana Vranes, Jason Park, Jay Ma-  
685 hadeokar, Jeet Shah, Jelmer van der Linde, Jennifer Billock, Jenny Hong, Jenya Lee, Jeremy Fu,  
686 Jianfeng Chi, Jianyu Huang, Jiawen Liu, Jie Wang, Jiecao Yu, Joanna Bitton, Joe Spisak, Jong-  
687 soo Park, Joseph Rocca, Joshua Johnstun, Joshua Saxe, Junteng Jia, Kalyan Vasuden Alwala,  
688 Karthik Prasad, Kartikeya Upasani, Kate Plawiak, Ke Li, Kenneth Heafield, Kevin Stone, Khalid  
689 El-Arini, Krithika Iyer, Kshitiz Malik, Kuenley Chiu, Kunal Bhatta, Kushal Lakhotia, Lauren  
690 Rantala-Yeary, Laurens van der Maaten, Lawrence Chen, Liang Tan, Liz Jenkins, Louis Martin,  
691 Lovish Madaan, Lubo Malo, Lukas Blecher, Lukas Landzaat, Luke de Oliveira, Madeline Muzzi,  
692 Mahesh Pasupuleti, Mannat Singh, Manohar Paluri, Marcin Kardas, Maria Tsimpoukelli, Mathew  
693 Oldham, Mathieu Rita, Maya Pavlova, Melanie Kambadur, Mike Lewis, Min Si, Mitesh Kumar  
694 Singh, Mona Hassan, Naman Goyal, Narjes Torabi, Nikolay Bashlykov, Nikolay Bogoychev,  
695 Niladri Chatterji, Ning Zhang, Olivier Duchenne, Onur Çelebi, Patrick Alrassy, Pengchuan  
696 Zhang, Pengwei Li, Petar Vasic, Peter Weng, Prajjwal Bhargava, Pratik Dubal, Praveen Krishnan,  
697 Punit Singh Koura, Puxin Xu, Qing He, Qingxiao Dong, Ragavan Srinivasan, Raj Ganapathy, Ra-  
698 mon Calderer, Ricardo Silveira Cabral, Robert Stojnic, Roberta Raileanu, Rohan Maheswari, Ro-  
699 hit Girdhar, Rohit Patel, Romain Sauvestre, Ronnie Polidoro, Roshan Sumbaly, Ross Taylor, Ruan  
700 Silva, Rui Hou, Rui Wang, Saghar Hosseini, Sahana Chennabasappa, Sanjay Singh, Sean Bell,  
701 Seohyun Sonia Kim, Sergey Edunov, Shaoliang Nie, Sharan Narang, Sharath Rparathy, Sheng  
Shen, Shengye Wan, Shruti Bhosale, Shun Zhang, Simon Vandenhende, Soumya Batra, Spencer  
Whitman, Sten Sootla, Stephane Collot, Suchin Gururangan, Sydney Borodinsky, Tamar Herman,  
Tara Fowler, Tarek Sheasha, Thomas Georgiou, Thomas Scialom, Tobias Speckbacher, Todor Mi-  
haylov, Tong Xiao, Ujjwal Karn, Vedanuj Goswami, Vibhor Gupta, Vignesh Ramanathan, Viktor

702 Kerkez, Vincent Gonguet, Virginie Do, Vish Vogeti, Vitor Albiero, Vladan Petrovic, Weiwei  
703 Chu, Wenhan Xiong, Wenyin Fu, Whitney Meers, Xavier Martinet, Xiaodong Wang, Xiaofang  
704 Wang, Xiaoqing Ellen Tan, Xide Xia, Xinfeng Xie, Xuchao Jia, Xuwei Wang, Yaelle Gold-  
705 schlag, Yashesh Gaur, Yasmine Babaei, Yi Wen, Yiwen Song, Yuchen Zhang, Yue Li, Yuning  
706 Mao, Zacharie Delpierre Coudert, Zheng Yan, Zhengxing Chen, Zoe Papanikos, Aaditya Singh,  
707 Aayushi Srivastava, Abha Jain, Adam Kelsey, Adam Shajnfeld, Adithya Gangidi, Adolfo Victoria,  
708 Ahuva Goldstand, Ajay Menon, Ajay Sharma, Alex Boesenberg, Alexei Baevski, Allie Feinstein,  
709 Amanda Kallet, Amit Sangani, Amos Teo, Anam Yunus, Andrei Lupu, Andres Alvarado, An-  
710 drew Caples, Andrew Gu, Andrew Ho, Andrew Poulton, Andrew Ryan, Ankit Ramchandani, An-  
711 nie Dong, Annie Franco, Anuj Goyal, Aparajita Saraf, Arkabandhu Chowdhury, Ashley Gabriel,  
712 Ashwin Bharambe, Assaf Eisenman, Azadeh Yazdan, Beau James, Ben Maurer, Benjamin Leon-  
713 hardi, Bernie Huang, Beth Loyd, Beto De Paola, Bhargavi Paranjape, Bing Liu, Bo Wu, Boyu  
714 Ni, Braden Hancock, Bram Wasti, Brandon Spence, Brani Stojkovic, Brian Gamido, Britt Mon-  
715 talvo, Carl Parker, Carly Burton, Catalina Mejia, Ce Liu, Changhan Wang, Changkyu Kim, Chao  
716 Zhou, Chester Hu, Ching-Hsiang Chu, Chris Cai, Chris Tindal, Christoph Feichtenhofer, Cynthia  
717 Gao, Damon Civin, Dana Beaty, Daniel Kreymer, Daniel Li, David Adkins, David Xu, Davide  
718 Testuggine, Delia David, Devi Parikh, Diana Liskovich, Didem Foss, Dingkan Wang, Duc Le,  
719 Dustin Holland, Edward Dowling, Eissa Jamil, Elaine Montgomery, Eleonora Presani, Emily  
720 Hahn, Emily Wood, Eric-Tuan Le, Erik Brinkman, Esteban Arcaute, Evan Dunbar, Evan Smoth-  
721 ers, Fei Sun, Felix Kreuk, Feng Tian, Filippos Kokkinos, Firat Ozgenel, Francesco Caggioni,  
722 Frank Kanayet, Frank Seide, Gabriela Medina Florez, Gabriella Schwarz, Gada Badeer, Georgia  
723 Swee, Gil Halpern, Grant Herman, Grigory Sizov, Guangyi, Zhang, Guna Lakshminarayanan,  
724 Hakan Inan, Hamid Shojanazeri, Han Zou, Hannah Wang, Hanwen Zha, Haroun Habeeb, Harri-  
725 son Rudolph, Helen Suk, Henry Aspegren, Hunter Goldman, Hongyuan Zhan, Ibrahim Damlaj,  
726 Igor Molybog, Igor Tufanov, Ilias Leontiadis, Irina-Elena Veliche, Itai Gat, Jake Weissman, James  
727 Geboski, James Kohli, Janice Lam, Japhet Asher, Jean-Baptiste Gaya, Jeff Marcus, Jeff Tang, Jen-  
728 nifer Chan, Jenny Zhen, Jeremy Reizenstein, Jeremy Teboul, Jessica Zhong, Jian Jin, Jingyi Yang,  
729 Joe Cummings, Jon Carvill, Jon Shepard, Jonathan McPhie, Jonathan Torres, Josh Ginsburg, Jun-  
730 jie Wang, Kai Wu, Kam Hou U, Karan Saxena, Kartikay Khandelwal, Katayoun Zand, Kathy  
731 Matosich, Kaushik Veeraraghavan, Kelly Michelena, Keqian Li, Kiran Jagadeesh, Kun Huang,  
732 Kunal Chawla, Kyle Huang, Lailin Chen, Lakshya Garg, Lavender A, Leandro Silva, Lee Bell,  
733 Lei Zhang, Liangpeng Guo, Licheng Yu, Liron Moshkovich, Luca Wehrstedt, Madian Khabsa,  
734 Manav Avalani, Manish Bhatt, Martynas Mankus, Matan Hasson, Matthew Lennie, Matthias  
735 Reso, Maxim Groshev, Maxim Naumov, Maya Lathi, Meghan Keneally, Miao Liu, Michael L.  
736 Seltzer, Michal Valko, Michelle Restrepo, Mihir Patel, Mik Vyatskov, Mikayel Samvelyan, Mike  
737 Clark, Mike Macey, Mike Wang, Miquel Jubert Hermoso, Mo Metanat, Mohammad Rastegari,  
738 Munish Bansal, Nandhini Santhanam, Natascha Parks, Natasha White, Navyata Bawa, Nayan  
739 Singhal, Nick Egebo, Nicolas Usunier, Nikhil Mehta, Nikolay Pavlovich Laptev, Ning Dong,  
740 Norman Cheng, Oleg Chernoguz, Olivia Hart, Omkar Salpekar, Ozlem Kalinli, Parkin Kent,  
741 Parth Parekh, Paul Saab, Pavan Balaji, Pedro Rittner, Philip Bontrager, Pierre Roux, Piotr Dollar,  
742 Polina Zvyagina, Prashant Ratanchandani, Pritish Yuvraj, Qian Liang, Rachad Alao, Rachel Ro-  
743 driguez, Rafi Ayub, Raghotham Murthy, Raghu Nayani, Rahul Mitra, Rangaprabhu Parthasarathy,  
744 Raymond Li, Rebekkah Hogan, Robin Battey, Rocky Wang, Russ Howes, Ruty Rinott, Sachin  
745 Mehta, Sachin Siby, Sai Jayesh Bondu, Samyak Datta, Sara Chugh, Sara Hunt, Sargun Dhillon,  
746 Sasha Sidorov, Satadru Pan, Saurabh Mahajan, Saurabh Verma, Seiji Yamamoto, Sharadh Ra-  
747 maswamy, Shaun Lindsay, Shaun Lindsay, Sheng Feng, Shenghao Lin, Shengxin Cindy Zha,  
748 Shishir Patil, Shiva Shankar, Shuqiang Zhang, Shuqiang Zhang, Sinong Wang, Sneha Agarwal,  
749 Soji Sajuyigbe, Soumith Chintala, Stephanie Max, Stephen Chen, Steve Kehoe, Steve Satter-  
750 field, Sudarshan Govindaprasad, Sumit Gupta, Summer Deng, Sungmin Cho, Sunny Virk, Suraj  
751 Subramanian, Sy Choudhury, Sydney Goldman, Tal Remez, Tamar Glaser, Tamara Best, Thilo  
752 Koehler, Thomas Robinson, Tianhe Li, Tianjun Zhang, Tim Matthews, Timothy Chou, Tzook  
753 Shaked, Varun Vontimitta, Victoria Ajayi, Victoria Montanez, Vijai Mohan, Vinay Satish Ku-  
754 mar, Vishal Mangla, Vlad Ionescu, Vlad Poenaru, Vlad Tiberiu Mihalescu, Vladimir Ivanov,  
755 Wei Li, Wenchen Wang, Wenwen Jiang, Wes Bouaziz, Will Constable, Xiaocheng Tang, Xiao-  
756 jian Wu, Xiaolan Wang, Xilun Wu, Xinbo Gao, Yaniv Kleinman, Yanjun Chen, Ye Hu, Ye Jia,  
757 Ye Qi, Yenda Li, Yilin Zhang, Ying Zhang, Yossi Adi, Youngjin Nam, Yu, Wang, Yu Zhao,  
758 Yuchen Hao, Yundi Qian, Yunlu Li, Yuzi He, Zach Rait, Zachary DeVito, Zef Rosnbrick, Zhao-  
759 duo Wen, Zhenyu Yang, Zhiwei Zhao, and Zhiyu Ma. The llama 3 herd of models, 2024. URL  
<https://arxiv.org/abs/2407.21783>.



- 756 Zhengfu He, Wentao Shu, Xuyang Ge, Lingjie Chen, Junxuan Wang, Yunhua Zhou, Frances Liu,  
757 Qipeng Guo, Xuanjing Huang, Zuxuan Wu, Yu-Gang Jiang, and Xipeng Qiu. Llama scope:  
758 Extracting millions of features from llama-3.1-8b with sparse autoencoders, 2024. URL <https://arxiv.org/abs/2410.20526>.  
759
- 760 Stefan Heimersheim and Neel Nanda. How to use and interpret activation patching. *Arxiv*, 2024.  
761 URL <https://arxiv.org/abs/2404.15255>.  
762
- 763 Jordan Hoffmann, Sebastian Borgeaud, Arthur Mensch, Elena Buchatskaya, Trevor Cai, Eliza  
764 Rutherford, Diego de Las Casas, Lisa Anne Hendricks, Johannes Welbl, Aidan Clark, Thomas  
765 Hennigan, Eric Noland, Katherine Millican, George van den Driessche, Bogdan Damoc, Au-  
766 relia Guy, Simon Osindero, Karén Simonyan, Erich Elsen, Oriol Vinyals, Jack Rae, and  
767 Laurent Sifre. An empirical analysis of compute-optimal large language model training.  
768 In S. Koyejo, S. Mohamed, A. Agarwal, D. Belgrave, K. Cho, and A. Oh (eds.), *Ad-  
769 vances in Neural Information Processing Systems*, volume 35, pp. 30016–30030. Curran As-  
770 sociates, Inc., 2022. URL [https://proceedings.neurips.cc/paper\\_files/paper/2022/  
771 hash/c1e2faff6f588870935f114ebe04a3e5-Abstract-Conference.html](https://proceedings.neurips.cc/paper_files/paper/2022/hash/c1e2faff6f588870935f114ebe04a3e5-Abstract-Conference.html).
- 772 Lei Huang, Weijiang Yu, Weitao Ma, Weihong Zhong, Zhangyin Feng, Haotian Wang, Qianglong  
773 Chen, Weihua Peng, Xiaocheng Feng, Bing Qin, and Ting Liu. A survey on hallucination in large  
774 language models: Principles, taxonomy, challenges, and open questions, 2023. URL <https://arxiv.org/abs/2311.05232>.  
775
- 776 Samyak Jain, Robert Kirk, Ekdeep Singh Lubana, Robert P. Dick, Hidenori Tanaka, Tim Rock-  
777 täschel, Edward Grefenstette, and David Krueger. Mechanistically analyzing the effects of fine-  
778 tuning on procedurally defined tasks. In *The Twelfth International Conference on Learning Rep-  
779 resentations*, 2024. URL <https://openreview.net/forum?id=A0HKeK14N1>.  
780
- 781 Ziwei Ji, Nayeon Lee, Rita Frieske, Tiezheng Yu, Dan Su, Yan Xu, Etsuko Ishii, Ye Jin Bang,  
782 Andrea Madotto, and Pascale Fung. Survey of hallucination in natural language generation. *ACM  
783 Computing Surveys*, 55(12), mar 2023. ISSN 0360-0300. doi: 10.1145/3571730. URL <https://doi.org/10.1145/3571730>.  
784
- 785 Nitish Joshi, Javier Rando, Abulhair Saparov, Najoung Kim, and He He. Personas as a way to model  
786 truthfulness in language models, 2024. URL <https://arxiv.org/abs/2310.18168>.
- 787 Connor Kissane, Robert Krzyzanowski, Arthur Conmy, and Neel Nanda. Base llms refuse too.  
788 *LessWrong*, 2024. URL [https://www.alignmentforum.org/posts/YWo2cKJg7Lg8xWjj/  
789 base-llms-refuse-too](https://www.alignmentforum.org/posts/YWo2cKJg7Lg8xWjj/base-llms-refuse-too).  
790
- 791 Jannik Kossen, Jiatong Han, Muhammed Razzak, Lisa Schut, Shreshth Malik, and Yarin Gal. Se-  
792 mantic entropy probes: Robust and cheap hallucination detection in llms, 2024. URL <https://arxiv.org/abs/2406.15927>.  
793
- 794 Robert Krzyzanowski, Connor Kissane, Arthur Conmy, and Neel Nanda. We in-  
795 spected every head in GPT-2 small using saes so you don’t have to. *AI Align-  
796 ment Forum*, 2024. URL [https://www.alignmentforum.org/posts/xmegeW5mqiBsvoaim/  
797 we-inspected-every-head-in-gpt-2-small-using-saes-so-you-don](https://www.alignmentforum.org/posts/xmegeW5mqiBsvoaim/we-inspected-every-head-in-gpt-2-small-using-saes-so-you-don).
- 798 Kenneth Li, Oam Patel, Fernanda Viégas, Hanspeter Pfister, and Martin Wattenberg. Inference-time  
799 intervention: Eliciting truthful answers from a language model. In *Thirty-seventh Conference  
800 on Neural Information Processing Systems*, 2023. URL [https://openreview.net/forum?id=  
801 aLLuYpn83y](https://openreview.net/forum?id=aLLuYpn83y).  
802
- 803 Tom Lieberum, Senthooran Rajamanoharan, Arthur Conmy, Lewis Smith, Nicolas Sonnerat, Vikrant  
804 Varma, János Kramár, Anca Dragan, Rohin Shah, and Neel Nanda. Gemma scope: Open sparse  
805 autoencoders everywhere all at once on gemma 2. *ArXiv*, 2024. URL [https://arxiv.org/abs/  
806 2408.05147](https://arxiv.org/abs/2408.05147).
- 807 Johnny Lin and Joseph Bloom. Announcing neuronpedia: Platform for  
808 accelerating research into sparse autoencoders. AI Alignment Forum,  
809 2024. URL [https://www.alignmentforum.org/posts/BaEQoxHhWPrkinmxd/  
announcing-neuronpedia-platform-for-accelerating-research](https://www.alignmentforum.org/posts/BaEQoxHhWPrkinmxd/announcing-neuronpedia-platform-for-accelerating-research).

- 810 Samuel Marks and Max Tegmark. The geometry of truth: Emergent linear structure in large language  
811 model representations of true/false datasets, 2023. URL <https://arxiv.org/abs/2310.06824>.
- 812
- 813 Samuel Marks, Can Rager, Eric J. Michaud, Yonatan Belinkov, David Bau, and Aaron Mueller.  
814 Sparse feature circuits: Discovering and editing interpretable causal graphs in language models.  
815 *ArXiv*, 2024. URL <https://arxiv.org/abs/2403.19647>.
- 816 Kevin Meng, David Bau, Alex Andonian, and Yonatan Belinkov. Locating and editing factual as-  
817 sociations in GPT. In S. Koyejo, S. Mohamed, A. Agarwal, D. Belgrave, K. Cho, and A. Oh  
818 (eds.), *Advances in Neural Information Processing Systems*, volume 35, pp. 17359–17372. Cur-  
819 ran Associates, Inc., 2022a. URL [https://proceedings.neurips.cc/paper\\_files/paper/](https://proceedings.neurips.cc/paper_files/paper/2022/hash/6f1d43d5a82a37e89b0665b33bf3a182-Abstract-Conference.html)  
820 [2022/hash/6f1d43d5a82a37e89b0665b33bf3a182-Abstract-Conference.html](https://proceedings.neurips.cc/paper_files/paper/2022/hash/6f1d43d5a82a37e89b0665b33bf3a182-Abstract-Conference.html).
- 821 Kevin Meng, David Bau, Alex Andonian, and Yonatan Belinkov. Locating and editing fact-  
822 ual associations in GPT. *Advances in Neural Information Processing Systems*, 36, 2022b.  
823 arXiv:2202.05262.
- 824
- 825 Tomas Mikolov, Ilya Sutskever, Kai Chen, Greg S Corrado, and Jeff Dean. Distributed represen-  
826 tations of words and phrases and their compositionality. In C.J. Burges, L. Bottou, M. Welling,  
827 Z. Ghahramani, and K.Q. Weinberger (eds.), *Advances in Neural Information Processing Sys-*  
828 *tems*, volume 26. Curran Associates, Inc., 2013. URL [https://proceedings.neurips.cc/](https://proceedings.neurips.cc/paper_files/paper/2013/hash/9aa42b31882ec039965f3c4923ce901b-Abstract.html)  
829 [paper\\_files/paper/2013/hash/9aa42b31882ec039965f3c4923ce901b-Abstract.html](https://proceedings.neurips.cc/paper_files/paper/2013/hash/9aa42b31882ec039965f3c4923ce901b-Abstract.html).
- 830 Shervin Minaee, Tomas Mikolov, Narjes Nikzad, Meysam Chenaghlu, Richard Socher, Xavier Am-  
831 atriain, and Jianfeng Gao. Large language models: A survey, 2024. URL [https://arxiv.org/](https://arxiv.org/abs/2402.06196)  
832 [abs/2402.06196](https://arxiv.org/abs/2402.06196).
- 833 Neel Nanda, Senthoran Rajamanoharan, János Kramár, and Rohin Shah. Fact find-  
834 ing: Attempting to reverse-engineer factual recall on the neuron level. *AI Align-*  
835 *ment Forum*, 2023. URL [https://www.alignmentforum.org/posts/iGwZTHWb6DFY3sKB/](https://www.alignmentforum.org/posts/iGwZTHWb6DFY3sKB/fact-finding-attempting-to-reverse-engineer-factual-recall)  
836 [fact-finding-attempting-to-reverse-engineer-factual-recall](https://www.alignmentforum.org/posts/iGwZTHWb6DFY3sKB/fact-finding-attempting-to-reverse-engineer-factual-recall).
- 837
- 838 Bruno A. Olshausen and David J. Field. Sparse coding with an overcomplete basis set: A strategy  
839 employed by v1? *Vision Research*, 37(23):3311–3325, 1997. ISSN 0042-6989. doi: [https://](https://doi.org/10.1016/S0042-6989(97)00169-7)  
840 [doi.org/10.1016/S0042-6989\(97\)00169-7](https://doi.org/10.1016/S0042-6989(97)00169-7). URL [https://www.sciencedirect.com/science/](https://www.sciencedirect.com/science/article/pii/S0042698997001697)  
841 [article/pii/S0042698997001697](https://www.sciencedirect.com/science/article/pii/S0042698997001697).
- 842 Kiho Park, Yo Joong Choe, and Victor Veitch. The linear representation hypothesis and the geometry  
843 of large language models. *Arxiv*, 2023. URL <https://arxiv.org/abs/2311.03658>.
- 844 Judea Pearl. *Causality*. Cambridge University Press, 2 edition, 2009. doi: 10.1017/  
845 [CBO9780511803161](https://doi.org/10.1017/CBO9780511803161).
- 846
- 847 Guilherme Penedo, Hynek Kydlíček, Loubna Ben allal, Anton Lozhkov, Margaret Mitchell, Colin  
848 Raffel, Leandro Von Werra, and Thomas Wolf. The fineweb datasets: Decanting the web for the  
849 finest text data at scale, 2024. URL <https://arxiv.org/abs/2406.17557>.
- 850 Nikhil Prakash, Tamar Rott Shaham, Tal Haklay, Yonatan Belinkov, and David Bau. Fine-tuning  
851 enhances existing mechanisms: A case study on entity tracking. *arXiv*, 2024. URL [https://](https://arxiv.org/abs/2402.14811)  
852 [arxiv.org/abs/2402.14811](https://arxiv.org/abs/2402.14811).
- 853 Alec Radford, Jeff Wu, Rewon Child, David Luan, Dario Amodei, and Ilya Sutskever.  
854 Language models are unsupervised multitask learners. *OpenAI Blog*, 2019. URL  
855 [https://d4mucfpksyw.cloudfront.net/better-language-models/language\\_models\\_](https://d4mucfpksyw.cloudfront.net/better-language-models/language_models_are_unsupervised_multitask_learners.pdf)  
856 [are\\_unsupervised\\_multitask\\_learners.pdf](https://d4mucfpksyw.cloudfront.net/better-language-models/language_models_are_unsupervised_multitask_learners.pdf).
- 857
- 858 Senthoran Rajamanoharan, Tom Lieberum, Nicolas Sonnerat, Arthur Conmy, Vikrant Varma, János  
859 Kramár, and Neel Nanda. Jumping ahead: Improving reconstruction fidelity with jumprelu sparse  
860 autoencoders, 2024. URL <https://arxiv.org/abs/2407.14435>.
- 861 Lee Sharkey, Dan Braun, and Beren Millidge. Taking features out of  
862 superposition with sparse autoencoders. *AI Alignment Forum*, 2022.  
863 URL [https://www.alignmentforum.org/posts/z6QQJbtpkEAX3Aojj/](https://www.alignmentforum.org/posts/z6QQJbtpkEAX3Aojj/interim-research-report-taking-features-out-of-superposition)  
[interim-research-report-taking-features-out-of-superposition](https://www.alignmentforum.org/posts/z6QQJbtpkEAX3Aojj/interim-research-report-taking-features-out-of-superposition).

- 864 Gemma Team, Morgane Riviere, Shreya Pathak, Pier Giuseppe Sessa, Cassidy Hardin, Surya Bhupatiraju, Léonard Hussenot, Thomas Mesnard, Bobak Shahriari, Alexandre Ramé, Johan Ferret, Peter Liu, Pouya Tafti, Abe Friesen, Michelle Casbon, Sabela Ramos, Ravin Kumar, Charline Le Lan, Sammy Jerome, Anton Tsitsulin, Nino Vieillard, Piotr Stanczyk, Sertan Girgin, Nikola Momchev, Matt Hoffman, Shantanu Thakoor, Jean-Bastien Grill, Behnam Neyshabur, Olivier Bachem, Alanna Walton, Aliaksei Severyn, Alicia Parrish, Aliya Ahmad, Allen Hutchison, Alvin Abdagic, Amanda Carl, Amy Shen, Andy Brock, Andy Coenen, Anthony Laforge, Antonia Paterson, Ben Bastian, Bilal Piot, Bo Wu, Brandon Royal, Charlie Chen, Chintu Kumar, Chris Perry, Chris Welty, Christopher A. Choquette-Choo, Danila Sinopalnikov, David Weinberger, Dimple Vijaykumar, Dominika Rogozińska, Dustin Herbison, Elisa Bandy, Emma Wang, Eric Noland, Erica Moreira, Evan Senter, Evgenii Eltyshev, Francesco Visin, Gabriel Rasskin, Gary Wei, Glenn Cameron, Gus Martins, Hadi Hashemi, Hanna Klimczak-Plucińska, Harleen Batra, Harsh Dhand, Ivan Nardini, Jacinda Mein, Jack Zhou, James Svensson, Jeff Stanway, Jetha Chan, Jin Peng Zhou, Joana Carrasqueira, Joana Iljazi, Jocelyn Becker, Joe Fernandez, Joost van Amersfoort, Josh Gordon, Josh Lipschultz, Josh Newlan, Ju yeong Ji, Kareem Mohamed, Kartikeya Badola, Kat Black, Katie Millican, Keelin McDonell, Kelvin Nguyen, Kiranbir Sodhia, Kish Greene, Lars Lowe Sjoesund, Lauren Usui, Laurent Sifre, Lena Heuermann, Leticia Lago, Lilly McNealus, Livio Baldini Soares, Logan Kilpatrick, Lucas Dixon, Luciano Martins, Machel Reid, Manvinder Singh, Mark Iverson, Martin Görner, Mat Velloso, Mateo Wirth, Matt Davidow, Matt Miller, Matthew Rahtz, Matthew Watson, Meg Risdal, Mehran Kazemi, Michael Moynihan, Ming Zhang, Minsuk Kahng, Minwoo Park, Mofi Rahman, Mohit Khatwani, Natalie Dao, Nenshad Bardoliwalla, Nesh Devanathan, Neta Dumai, Nilay Chauhan, Oscar Wahltinez, Pankil Botarda, Parker Barnes, Paul Barham, Paul Michel, Pengchong Jin, Petko Georgiev, Phil Culliton, Pradeep Kuppala, Ramona Comanescu, Ramona Merhej, Reena Jana, Reza Ardeshtir Rokni, Rishabh Agarwal, Ryan Mullins, Samaneh Saadat, Sara Mc Carthy, Sarah Perrin, Sébastien M. R. Arnold, Sebastian Krause, Shengyang Dai, Shruti Garg, Shruti Sheth, Sue Ronstrom, Susan Chan, Timothy Jordan, Ting Yu, Tom Eccles, Tom Hennigan, Tomas Kocisky, Tulsee Doshi, Vihan Jain, Vikas Yadav, Vilobh Meshram, Vishal Dharmadhikari, Warren Barkley, Wei Wei, Wenming Ye, Woohyun Han, Woosuk Kwon, Xiang Xu, Zhe Shen, Zhitao Gong, Zichuan Wei, Victor Cotruta, Phoebe Kirk, Anand Rao, Minh Giang, Ludovic Peran, Tris Warkentin, Eli Collins, Joelle Barral, Zoubin Ghahramani, Raia Hadsell, D. Sculley, Jeanine Banks, Anca Dragan, Slav Petrov, Oriol Vinyals, Jeff Dean, Demis Hassabis, Koray Kavukcuoglu, Clement Farabet, Elena Buchatskaya, Sebastian Borgeaud, Noah Fiedel, Armand Joulin, Kathleen Kenealy, Robert Dadashi, and Alek Andreev. Gemma 2: Improving open language models at a practical size. *ArXiv*, 2024. URL <https://arxiv.org/abs/2408.00118>.
- 897 Adly Templeton, Tom Conerly, Jonathan Marcus, Jack Lindsey, Trenton Bricken, Brian Chen, Adam Pearce, Craig Citro, Emmanuel Ameisen, Andy Jones, Hoagy Cunningham, Nicholas L Turner, Callum McDougall, Monte MacDiarmid, C. Daniel Freeman, Theodore R. Sumers, Edward Rees, Joshua Batson, Adam Jermyn, Shan Carter, Chris Olah, and Tom Henighan. Scaling monosemanticity: Extracting interpretable features from claude 3 sonnet. *Transformer Circuits Thread*, 2024. URL <https://transformer-circuits.pub/2024/scaling-monosemanticity/index.html>.
- 904 Curt Tigges, Oskar John Hollinsworth, Atticus Geiger, and Neel Nanda. Linear representations of sentiment in large language models. *Arxiv*, 2023. URL <https://arxiv.org/abs/2310.15154>.
- 906 Alexander Matt Turner, Lisa Thiergart, David Udell, Gavin Leech, Ulisse Mini, and Monte MacDiarmid. Activation addition: Steering language models without optimization, 2023.
- 909 Neeraj Varshney, Wenlin Yao, Hongming Zhang, Jianshu Chen, and Dong Yu. A stitch in time saves nine: Detecting and mitigating hallucinations of llms by validating low-confidence generation, 2023. URL <https://arxiv.org/abs/2307.03987>.
- 913 Jesse Vig, Sebastian Gehrmann, Yonatan Belinkov, Sharon Qian, Daniel Nevo, Yaron Singer, and Stuart Shieber. Investigating gender bias in language models using causal mediation analysis. In H. Larochelle, M. Ranzato, R. Hadsell, M.F. Balcan, and H. Lin (eds.), *Advances in Neural Information Processing Systems*, volume 33, pp. 12388–12401. Curran Associates, Inc., 2020. URL <https://proceedings.neurips.cc/paper/2020/hash/92650b2e92217715fe312e6fa7b90d82-Abstract.html>.

918 Denny Vrandečić and Markus Krötzsch. Wikidata: A free collaborative knowledgebase. *ACM*,  
919 2024. URL <https://cacm.acm.org/research/wikidata/>.  
920

921 Kevin Ro Wang, Alexandre Variengien, Arthur Conmy, Buck Shlegeris, and Jacob Steinhardt. Inter-  
922 pretability in the wild: a circuit for indirect object identification in GPT-2 small. In *The Eleventh*  
923 *International Conference on Learning Representations*, 2023. URL [https://openreview.net/](https://openreview.net/forum?id=NpsVSN6o4u1)  
924 [forum?id=NpsVSN6o4u1](https://openreview.net/forum?id=NpsVSN6o4u1).

925 Gal Yona, Roei Aharoni, and Mor Geva. Can large language models faithfully express their intrinsic  
926 uncertainty in words?, 2024. URL <https://arxiv.org/abs/2405.16908>.  
927

928 Lei Yu, Meng Cao, Jackie Chi Kit Cheung, and Yue Dong. Mechanistic understanding and mitiga-  
929 tion of language model non-factual hallucinations. *arXiv*, 2024. URL [https://arxiv.org/abs/](https://arxiv.org/abs/2403.18167)  
930 [2403.18167](https://arxiv.org/abs/2403.18167).

931 Qinan Yu, Jack Merullo, and Ellie Pavlick. Characterizing mechanisms for factual recall in language  
932 models, 2023. URL <https://arxiv.org/abs/2310.15910>.  
933

934 Mert Yuksekgonul, Varun Chandrasekaran, Erik Jones, Suriya Gunasekar, Ranjita Naik, Hamid  
935 Palangi, Ece Kamar, and Besmira Nushi. Attention satisfies: A constraint-satisfaction lens on  
936 factual errors of language models. In *The Twelfth International Conference on Learning Repre-*  
937 *sentations*, 2024. URL <https://openreview.net/forum?id=gfFVATffPd>.

938 Andy Zou, Long Phan, Sarah Chen, James Campbell, Phillip Guo, Richard Ren, Alexander  
939 Pan, Xuwang Yin, Mantas Mazeika, Ann-Kathrin Dombrowski, Shashwat Goel, Nathaniel Li,  
940 Michael J. Byun, Zifan Wang, Alex Mallen, Steven Basart, Sanmi Koyejo, Dawn Song, Matt  
941 Fredrikson, J. Zico Kolter, and Dan Hendrycks. Representation engineering: A top-down ap-  
942 proach to ai transparency. *Arxiv*, 2023. URL <https://arxiv.org/abs/2310.01405>.  
943  
944  
945  
946  
947  
948  
949  
950  
951  
952  
953  
954  
955  
956  
957  
958  
959  
960  
961  
962  
963  
964  
965  
966  
967  
968  
969  
970  
971

## A ENTITY DIVISION INTO KNOWN AND UNKNOWN

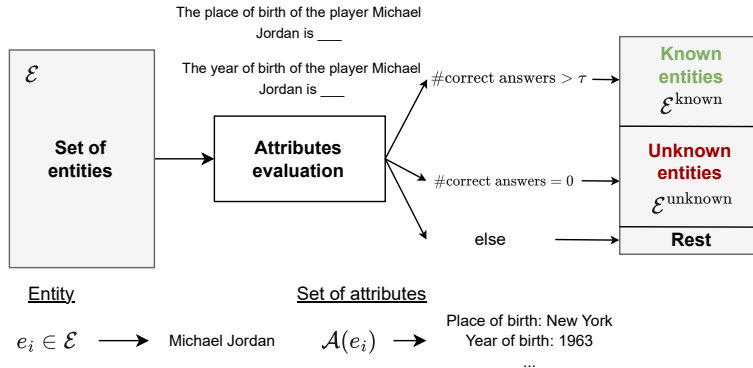


Figure 7: Pipeline for classifying entities as known or unknown. Each entity  $e_i \in \mathcal{E}$  is evaluated by querying the language model about a set of attributes  $\mathcal{A}(e_i)$ . Classification as known or unknown is based on the accuracy of the model’s responses. In this work we set the threshold  $\tau = 1$ .

Entity Type	Number of entities	Attributes
Player	7487	Birthplace, birthdate, teams played
Movie	10895	Director, screenwriter, release date, genre, duration, cast
City	7904	Country, population, elevation, coordinates
Song	8448	Artist, album, publication year, genre

Table 3: Entity types and attributes extracted from Wikidata.



## B ENTITY RECOGNITION LATENTS ON DIVERSE ENTITIES

1026  
1027  
1028  
1029  
1030  
1031  
1032  
1033  
1034  
1035  
1036  
1037  
1038  
1039  
1040  
1041  
1042  
1043  
1044  
1045  
1046  
1047  
1048  
1049  
1050  
1051  
1052  
1053  
1054  
1055  
1056  
1057  
1058  
1059  
1060  
1061  
1062  
1063  
1064  
1065  
1066  
1067  
1068  
1069  
1070  
1071  
1072  
1073  
1074  
1075  
1076  
1077  
1078  
1079

Known Entity Latent Activations	Unknown Entity Latent Activations
Many people use <b>Twitter</b> to share their thoughts.	Many people use Twitter to share their thoughts.
<b>L'Oréal</b> is a large cosmetics and beauty company.	L'Oréal is a large cosmetics and beauty company.
The <b>Mona Lisa</b> is displayed in the <b>Louvre</b> museum.	The Mona Lisa is displayed in the Louvre museum.
Many people use <b>Snapchat</b> for sharing photos and short videos.	Many people use Snapchat for sharing photos and short videos.
The <b>Acropolis</b> is an ancient citadel in <b>Athens</b> .	The Acropolis is an ancient citadel in Athens.
The <b>Galapagos Islands</b> are known for their unique wildlife.	The Galapagos Islands are known for their unique wildlife.
Many people use <b>Dropbox</b> for cloud storage.	Many people use Dropbox for cloud storage.
The <b>pyramids of Giza</b> were built by ancient <b>Egyptians</b> .	The pyramids of Giza were built by ancient Egyptians.
<b>Walmart</b> is the world's largest company by revenue.	Walmart is the world's largest company by revenue.
<b>FedEx</b> is a multinational delivery services company.	FedEx is a multinational delivery services company.
Many people use <b>Instagram</b> to share photos.	Many people use Instagram to share photos.
The <b>Neuschwanstein Castle</b> inspired Disney's <b>Sleeping Beauty Castle</b> .	The Neuschwanstein Castle inspired Disney's Sleeping Beauty Castle.
The theory of gravity was developed by Isaac <b>Newton</b> .	The theory of gravity was developed by Isaac Newton.
Sony <b>is</b> known for its electronics and entertainment products.	Sony is known for its electronics and entertainment products.
Many people use <b>Skype</b> for voice and video calls.	Many people use Skype for voice and video calls.
The Sistine <b>Chapel</b> is famous for its frescoes by <b>Michelangelo</b> .	The Sistine Chapel is famous for its frescoes by Michelangelo.
The <b>Andes</b> are the longest continental mountain range in the world.	The Andes are the longest continental mountain range in the world.
The theory of evolution was proposed by Charles <b>Darwin</b> .	The theory of evolution was proposed by Charles Darwin.
Many people use <b>Shopify</b> for e-commerce platforms.	Many people use Shopify for e-commerce platforms.
<b>Honda is</b> known for its motorcycles and automobiles.	Honda is known for its motorcycles and automobiles.

Table 4: Activations of Gemma 2 2B entity recognition latents on LLM generated data.

	<b>Known Entity Latent Activations</b>	<b>Unknown Entity Latent Activations</b>
1080		
1081		
1082	Druids commune with nature in the sacred grove of Elth <sup>al</sup> as.	Druids commune with nature in the sacred grove of El <sup>th</sup> al <sup>as</sup> .
1083		
1084	Adventurers seek the lost treasure of King Zephy <sup>ri</sup> on.	Adventurers seek the lost treasure of King Zep <sup>h</sup> yr <sup>io</sup> n.
1085		
1086	The Thaumaturge’s Guild specializes in Aether manipulation.	The Thaumaturge’s Guild specializes in Aether manipulation.
1087		
1088	The Vorp <sup>a</sup> l Blade was forged by the legendary Jabberwo <sup>ck</sup> .	The Vorp <sup>a</sup> l Bl <sup>a</sup> d <sup>e</sup> was forged by the legendary Jabberwo <sup>ck</sup> .
1089		
1090	The Hivemind of Xar <sup>z</sup> ith threatens galactic peace.	The Hivemind of Xar <sup>z</sup> ith threatens galactic peace.
1091		
1092	Travelers must appease the Stormcall <sup>e</sup> r to cross the Tempest Sea.	Travelers must appease the Stormcall <sup>e</sup> r to cross the Tempest S <sup>e</sup> a.
1093		
1094	Archaeologists unearthed artifacts from the Zanth <sup>a</sup> r civilization.	Archaeologists unearthed artifacts from the Zanth <sup>a</sup> r civilization.
1095		
1096	Sailors fear the treacherous waters of the Myrosk <sup>i</sup> an Sea.	Sailors fear the treacherous waters of the Myrosk <sup>i</sup> an S <sup>e</sup> a.
1097		
1098	Scientists studied the unique properties of Quixium alloy.	Scientists studied the unique properties of Quixium alloy.
1099		
1100	The Glibberthorn plant is known for its healing properties.	The Glibberthorn plant is known for its healing properties.
1101		
1102	The Voidwalker emerged from the Abyssal Rift.	The Voidwalker emerged from the Abyssal Rift.
1103		
1104	Alchemists seek to create the legendary Philosopher’s Stone.	Alchemists seek to create the legendary Philosopher’s Stone.
1105		
1106	Pilgrims seek enlightenment at the Temple of Ethereal Wisdom.	Pilgrims seek enlightenment at the Temple of Ethereal Wisdom.
1107		
1108	Pilots navigate through the treacherous Astral Maelstrom.	Pilots navigate through the treacherous Astral Maelstrom.
1109		
1110	Merchants trade rare gems in the bazaars of Khalin <sup>d</sup> or.	Merchants trade rare gems in the bazaars of Khalin <sup>d</sup> or.
1111		
1112	Scholars study ancient texts at the University of Arcanum.	Scholars study ancient texts at the University of Arcanum.
1113		
1114	The Vexnor device revolutionized quantum computing.	The Vexnor device revolutionized quantum computing.
1115		
1116	The Whispering Woods are guarded by the Sylvani.	The Whispering Woods are guarded by the Sylvani.
1117		
1118	The Ethereal Conclave governs the realm of spirits.	The Ethereal Conclave governs the realm of spirits.
1119		
1120	The Quantum Forge harnesses the power of Nullstone.	The Quantum Forge harnesses the power of Nullstone.

Table 5: Activations of Gemma 2 2B entity recognition latents on LLM generated data.

1121  
1122  
1123  
1124  
1125  
1126  
1127  
1128  
1129  
1130  
1131  
1132  
1133

## C GEMMA 2 9B LATENTS ACTIVATION FREQUENCIES ON KNOWN AND UNKNOWN PROMPTS

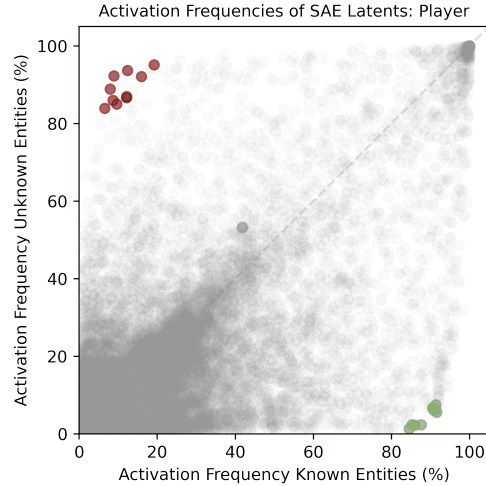


Figure 8: Activation frequencies of Gemma 2 9B SAE latents on known and unknown Prompts, in player entity type.

## D GEMMA 2 9B LAYERWISE EVOLUTION OF THE TOP 5 LATENTS

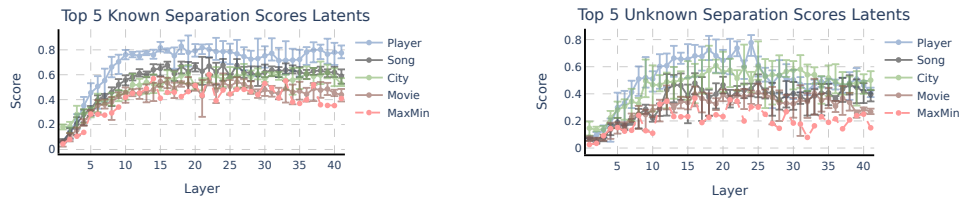


Figure 9: Gemma 2 9B layerwise evolution of the Top 5 latents, as measured by their known (left) and unknown (right) latent separation scores ( $s^{\text{known}}$  and  $s^{\text{unknown}}$ ). Error bars show maximum and minimum scores. MaxMin (red line) refers to the minimum separation score across entities of the best latent. This represents how entity-agnostic is the most general latent per layer. In both cases, middle layers provide the best-performing latents.

## E NORM RESIDUAL STREAMS

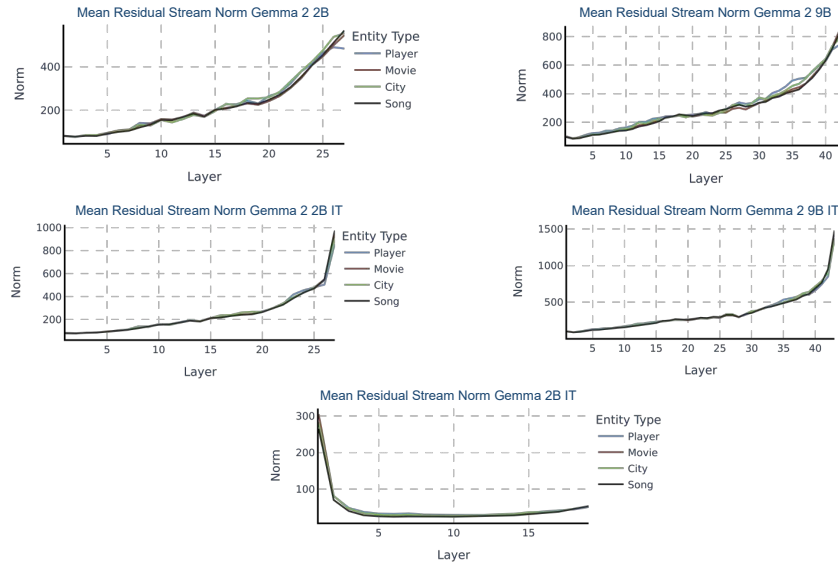


Figure 10: Norm of the residual streams of the last token of the entity across layers of the different Gemma models.

## F REFUSAL RATES GEMMA 2 9B

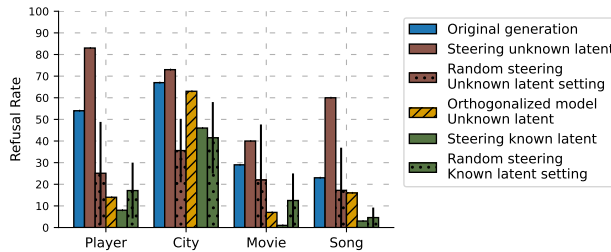


Figure 11: **Left:** Number of times Gemma 2 9B refuses to answer in 100 queries about unknown entities. We examine the unmodified original model, the model steered with the known entity latent and unknown entity latent, and the model with the unknown entity latent projected out of its weights (referred to as Orthogonalized model). The mean and standard deviation of steering with 10 random latents are shown for comparison. **Right:** This example illustrates the effect of steering with the unknown entity recognition latent. The steering induces the model to refuse to answer about a well-known basketball player.

## G EXAMPLE OF GENERATIONS STEERING WITH DIFFERENT COEFFICIENTS

<b>Question: Where was born the player Leo Barnhorst?</b>	
$\alpha$	<b>Generation</b>
0	Leo Barnhorst was born in <b>Berlin, Germany</b> .
100	Leo Barnhorst was born in <b>Germany</b> .
200	I do not have access to real-time information, including personal details like birthplaces.
300	I do not have access to real-time information, including personal details like birthplaces.
400	I couldn't find any information about a player named Leo Barnhorst.
500	I believe you're asking about <b>Leo Barnhorst</b> , a professional soccer player.
600	I'm unable to provide specific details about the birthplace of a player named Leo Barnhorst.
700	? Please provide me with the correct spelling of the player's name.
800	I believe you're asking about <b>Leo Barnhart</b> , a professional soccer player.
900	"I believe you're asking about <b>Leo Barnhart</b> , a professional soccer player.
1000	I believe you're asking about <b>Leo Barnhart</b> , a professional soccer player.
1100	Associate the player Leo Barnhart with the sport of <b>baseball</b> .
1200	criminator: I'm sorry, but I don't have access to real-time information, including personal details like birthplaces.

Table 6: Gemma 2 2B IT responses to ‘Where was born the player Leo Barnhorst?’ at different steering coefficient values,  $\alpha$  in Equation (4). Leo Barnhorst is unknown for Gemma 2 2B.



## H ACTIVATION PATCHING

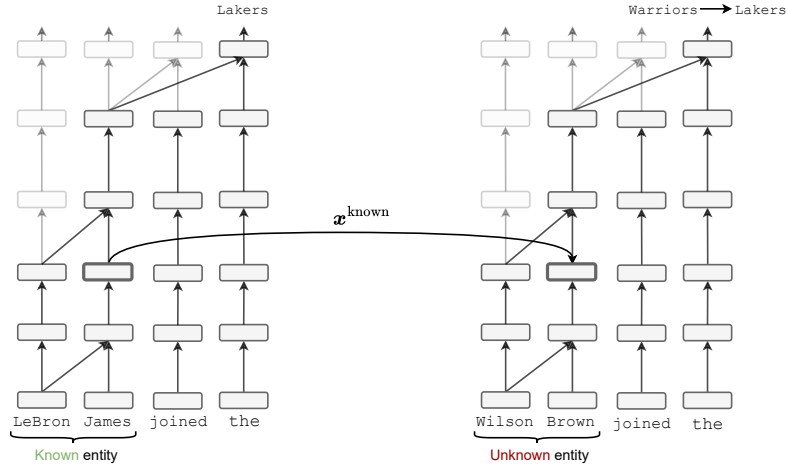


Figure 12: Activation Patching done over the residual stream.

Activation patching (Vig et al., 2020; Meng et al., 2022a; Geiger et al., 2020; Wang et al., 2023) is an intervention procedure performed during a forward pass. We consider a ‘clean’ input, which in our case is the prompt with a known entity (Figure 12 left). We compute an intermediate hidden state, e.g. the residual steam value at token James, as in Figure 12. Then, we patch this activation at the same site of the forward pass with the corrupted input. In this case, the corrupted input is a prompt with an unknown entity. We can express this intervention using the do-operator (Pearl, 2009) as  $f(\text{corr}|\text{do}(x^{\text{unknown}} \leftarrow x^{\text{known}}))$ . After the intervention is done, the forward pass continues and the model output is compared with the prediction with the corrupted input. In the experiments in Section 6 we measure the logit difference between the clean (Lakers) and the corrupted predictions (Warriors):

$$\frac{\text{logit}_{\text{Lakers-Warriors}}(\text{corr}|\text{do}(x^{\text{unknown}} \leftarrow x^{\text{known}}))}{\text{logit}_{\text{Lakers-Warriors}}(\text{clean})} \quad (13)$$

## I ACTIVATION PATCHING ON GEMMA 2 2B

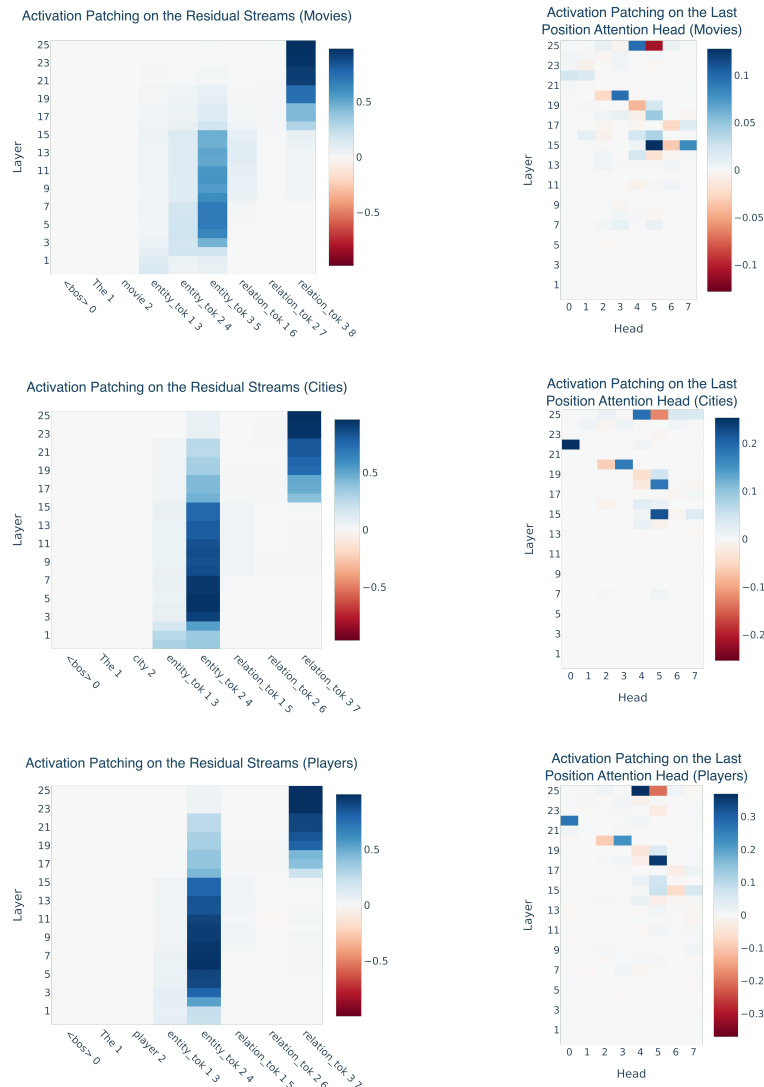


Figure 13: Gemma 2 2B activation patching results on movies (top), players (middle) and cities (bottom).

J ACTIVATION PATCHING ON GEMMA 2 9B

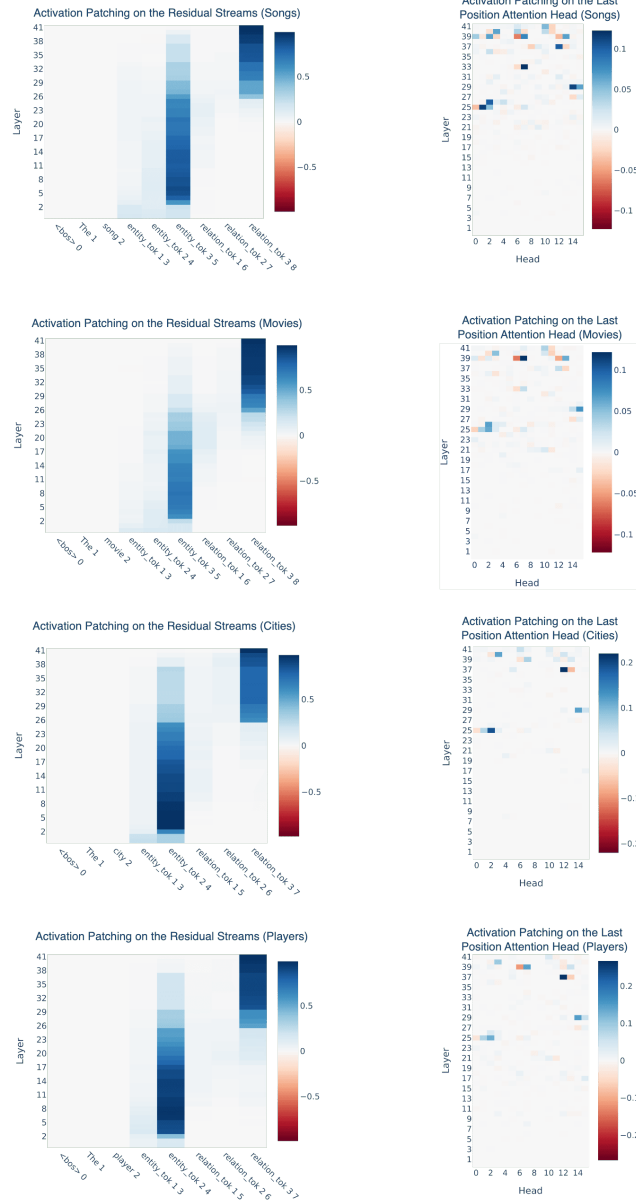


Figure 14: Gemma 2 9B activation patching results on. from top to bottom, song, movies, players and cities.

K ATTENTION TO LAST ENTITY TOKEN AFTER RANDOM LATENT STEERING

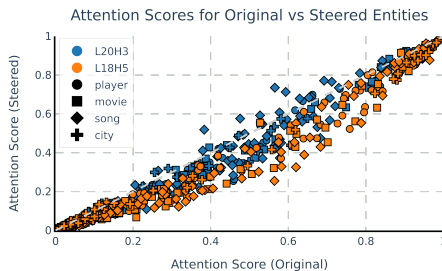


Figure 15: Comparison of attention scores to the last token of the entity after steering with a random SAE latent from Layer 15.

L ATTRIBUTE EXTRACTION HEADS EXAMPLES

Head	Entity	Extracted Attributes
L18H5	Kawhi Leonard	Clippers, Niagara, Raptors,
	Detmold	Westfalen, Lancaster, Volkswagen
	Boombastic	Jamaican, Reggae, Jamaica, Caribbean
L20H3	Kawhi Leonard	NBA, basketball, Clippers, Basketball
	Detmold	Germans, German, Germany, Westfalen
	Boombastic	reggae, Reggae, Jamaican, music, song

Table 7: Examples from the top tokens promoted by the attribute extraction heads L18H5 and L20H3 in Gemma 2 2B.

## M CHANGE OF ATTENTION SCORES TO ENTITIES AFTER STEERING

Gemma 2 2B (Figures 16 and 17), Gemma 2 9B (Figures 18 and 19) and Llama 3.1 8B (Figures 20 and 21) average attention scores to entity tokens after steering with the top known entity latents and top unknown entity latents. Error bars indicate standard deviation. For the known entity latent steering we use prompts with unknown entities, for the unknown entity latent steering we use prompts with known entities. The strength of the steering coefficient is  $\alpha = 100$  for Gemma models and  $\alpha = 20$  for Llama 3.1 8B. We show heads starting from layer the latent is found, and the steering is done.

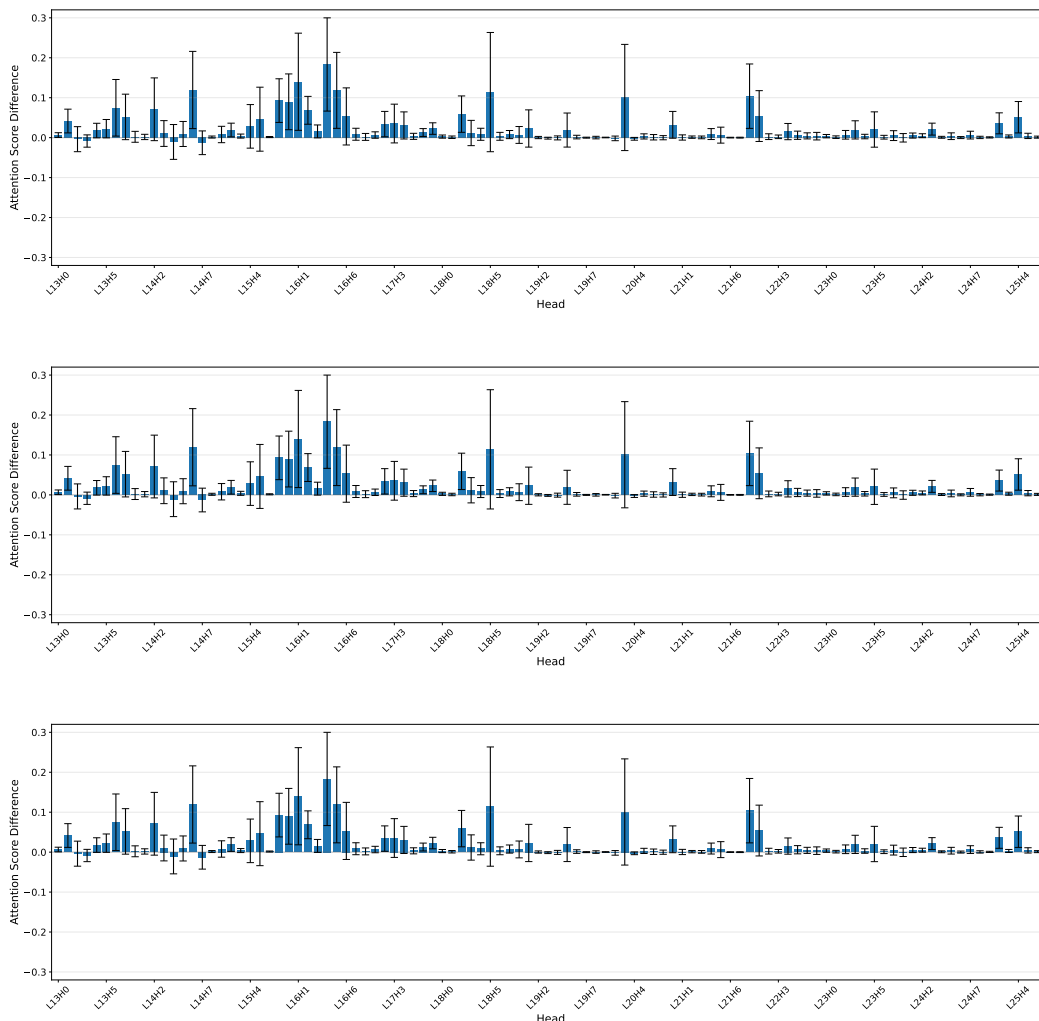


Figure 16: Aggregated attention scores to entity tokens per head in Gemma 2 2B. Steering is done with the top 3 known entity latents (from top to bottom).

We have assessed the statistical significance of attention score changes by comparing steering with entity recognition latents versus with random SAE latents using the same layer and steering coefficient. We conduct t-tests where the null hypothesis states that both steerings would yield identical mean attention scores differences across downstream attention heads. The alternative hypothesis is that known entity latents would increase mean attention scores, while unknown entity latents would decrease them. We tested against 10 different random SAE latents using 100 distinct prompts.

Results indicate that for Gemma 2 2B, Gemma 2 9B and Llama 3.1 8B, steering with the top known entity latent shows statistically significant larger average attention score when compared to random SAE latents on 10/10, 10/10 and 7/10 cases respectively. When steering with the top unknown entity

1566  
 1567  
 1568  
 1569  
 1570  
 1571  
 1572  
 1573  
 1574  
 1575  
 1576  
 1577  
 1578  
 1579  
 1580  
 1581  
 1582  
 1583  
 1584  
 1585  
 1586  
 1587  
 1588  
 1589  
 1590  
 1591  
 1592  
 1593  
 1594  
 1595  
 1596  
 1597  
 1598  
 1599  
 1600  
 1601  
 1602  
 1603  
 1604  
 1605  
 1606  
 1607  
 1608  
 1609  
 1610  
 1611  
 1612  
 1613  
 1614  
 1615  
 1616  
 1617  
 1618  
 1619

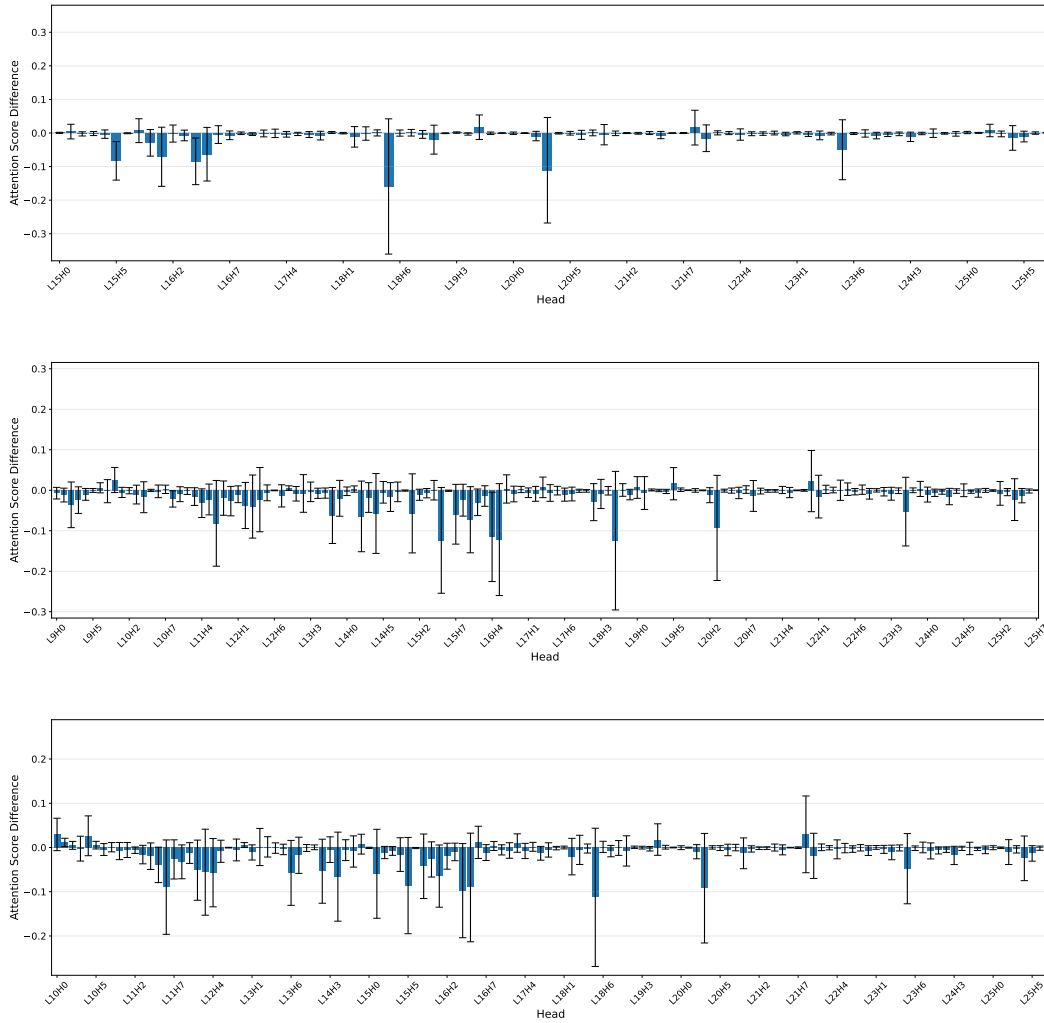


Figure 17: Aggregated attention scores to entity tokens per head in Gemma 2 2B. Steering is done with the top 3 unknown entity latents (from top to bottom).

latent it shows statistically significant lower average attention score when compared to random SAE latents on 9/10, 1/10 and 10/10 cases respectively. As shown in Figure 19 (top), Gemma 2 9B top unknown entity latent doesn't show strong reductions. However the second unknown entity latent shows significant differences in 9/10 tests.

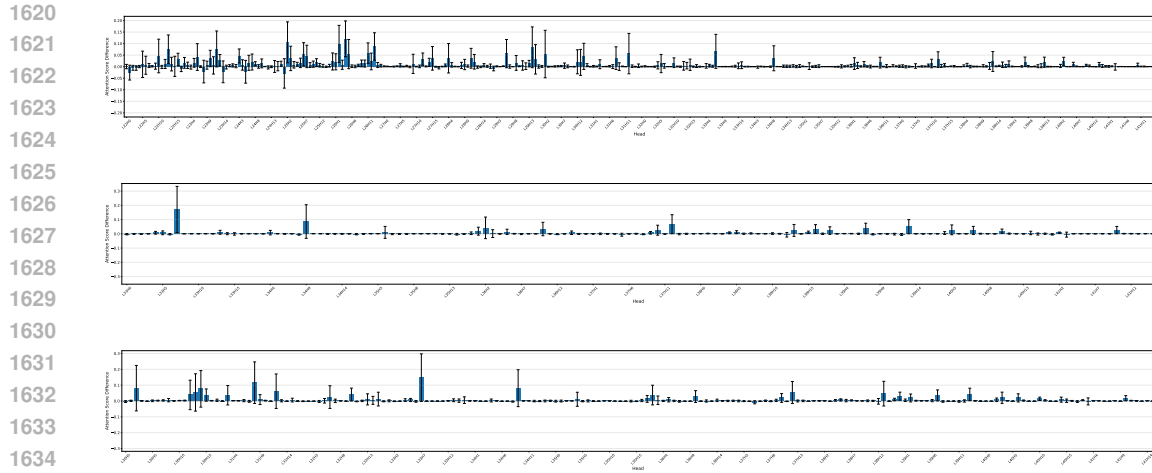


Figure 18: Aggregated attention scores to entity tokens per head in Gemma 2 9B. Steering is done with the top 3 known entity latents (from top to bottom).

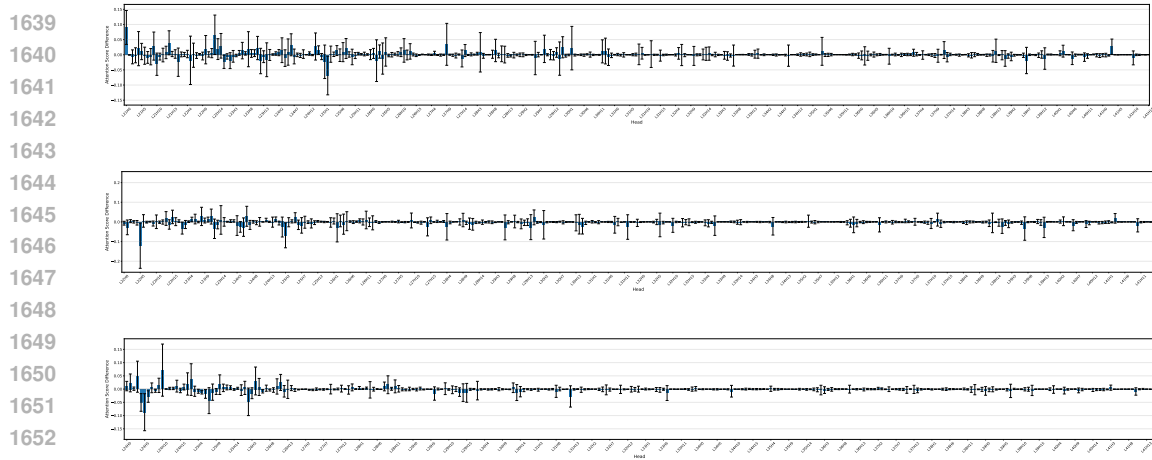


Figure 19: Aggregated attention scores to entity tokens per head in Gemma 2 9B. Steering is done with the top 3 unknown entity latents (from top to bottom).

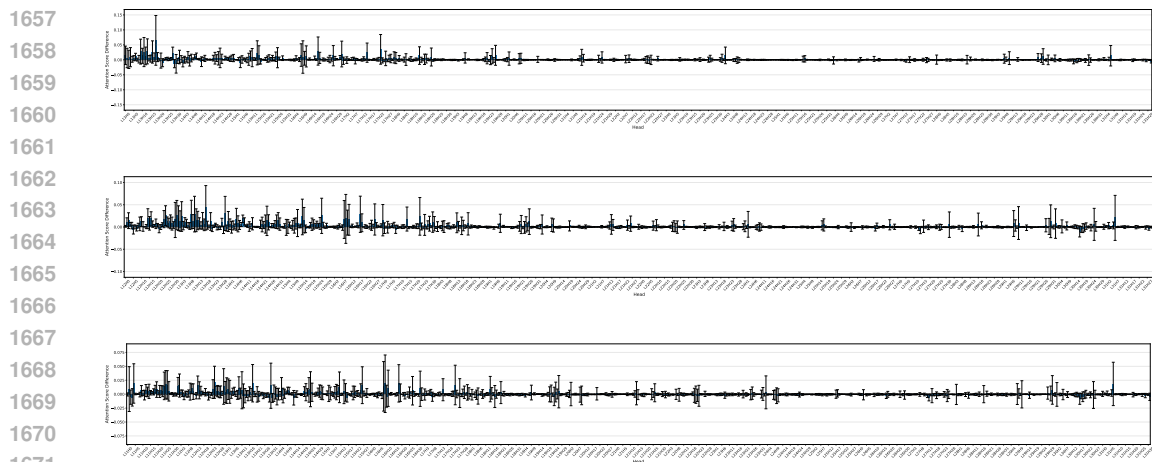


Figure 20: Aggregated attention scores to entity tokens per head in Llama 3.1 8B. Steering is done with the top 3 known entity latents (from top to bottom).

1674  
1675  
1676  
1677  
1678  
1679  
1680  
1681  
1682  
1683  
1684  
1685  
1686  
1687  
1688  
1689  
1690  
1691  
1692  
1693  
1694  
1695  
1696  
1697  
1698  
1699  
1700  
1701  
1702  
1703  
1704  
1705  
1706  
1707  
1708  
1709  
1710  
1711  
1712  
1713  
1714  
1715  
1716  
1717  
1718  
1719  
1720  
1721  
1722  
1723  
1724  
1725  
1726  
1727

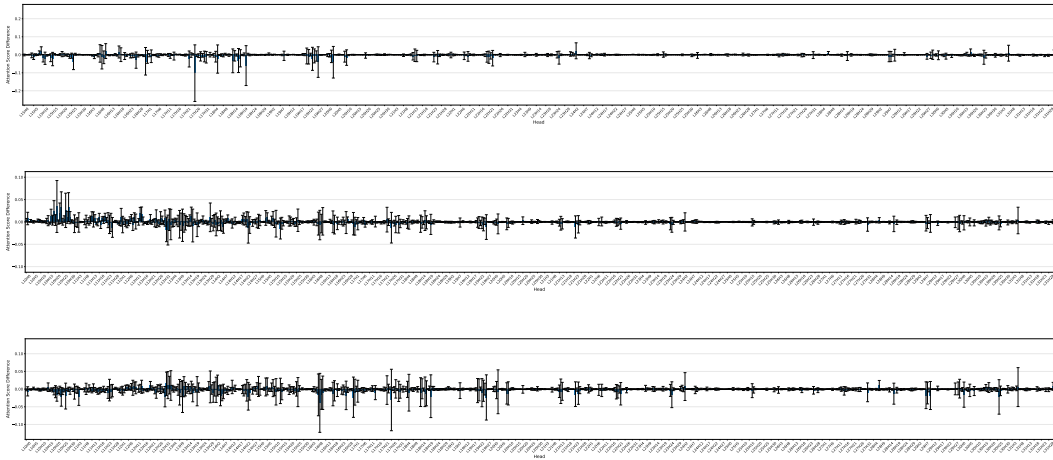


Figure 21: Aggregated attention scores to entity tokens per head in Llama 3.1 8B. Steering is done with the top 3 unknown entity latents (from top to bottom).



N GEMMA 2 9B SELF KNOWLEDGE REFLECTION

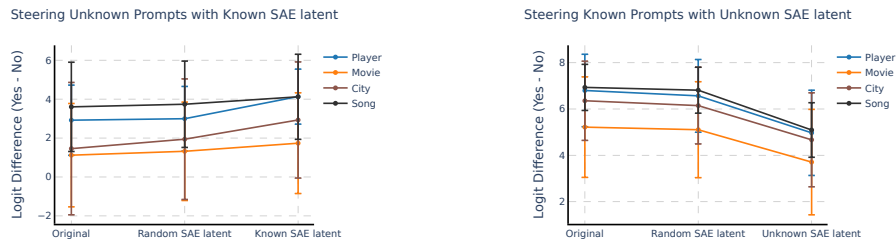


Figure 22: Gemma 2 9B Logit difference between “Yes” and “No” predictions on the question “Are you sure you know the {entity\_type} {entity\_name}? Answer yes or no.” after steering with unknown (left) and known (right) entity recognition latents..

O GEMMA 2 9B IT TOP ‘UNKNOWN’ LATENTS

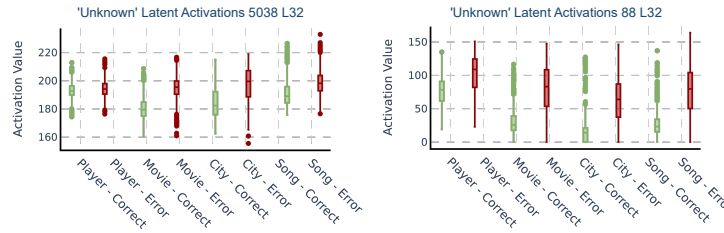


Figure 23: Top 2 Gemma 2 9B IT ‘unknown’ latents based on the t-statistic score.

P GEMMA 2B IT TOP ‘UNKNOWN’ LATENT WITH SEPARATED ERRORS BASED ON ENTITY TYPE

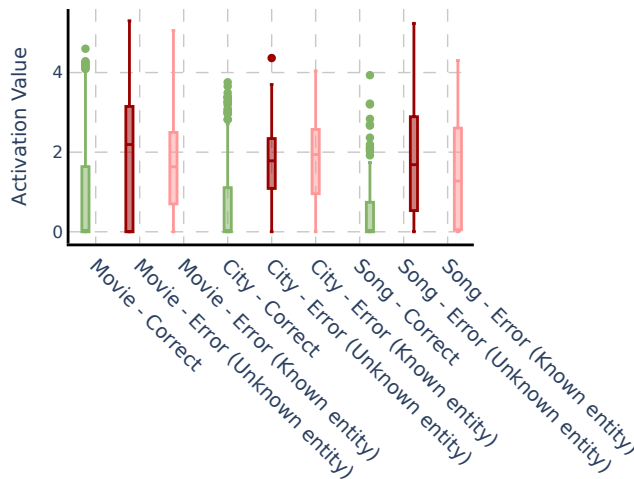


Figure 24: Top 2 Gemma 2B IT ‘unknown’ latent based on the t-statistic score, with errors divided into known and unknown entities.

## Q LLAMA 3.1 8B REPLICATION

We extend our experimental analysis to Llama 3.1 8B (Grattafiori et al., 2024), using the SAEs suite from LlamaScope (He et al., 2024), which offers per-layer pretrained SAEs. Following the methodology described in Section 3, we detect both known and unknown entity latents within the model. The distribution of the Top 5 latents across layers (Figure 25) exhibit consistent patterns with previous findings, with the most effective and generalizable latent representations concentrated in the intermediate layers.

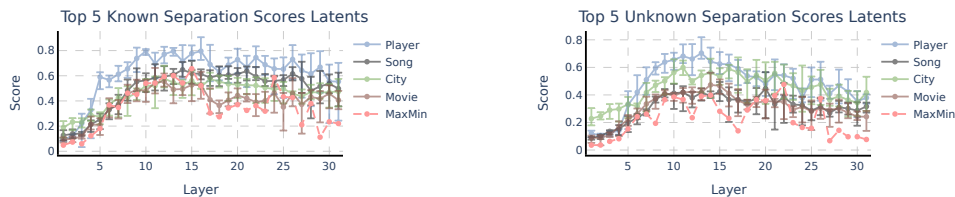


Figure 25: Llama 3.1 8B layerwise evolution of the Top 5 latents, as measured by their known (left) and unknown (right) latent separation scores. Error bars show maximum and minimum scores. MaxMin (red line) refers to the minimum separation score across entities of the best latent. This represents how entity-agnostic is the most general latent per layer. In both cases, middle layers provide the best-performing latents.

Steering experiments using the top unknown entity latent reveal increase refusal rates in the instruction-tuned model (Figure 26). Conversely, when we orthogonalize the model weights with respect to this direction, refusal rates decrease. Since the original model’s refusal rate on unknown entity prompts is high (Figure 26 left), we include the refusal rates on prompts with known entities (Figure 26 right). Notably, steering with the top known entity latent did not produce a corresponding decrease in refusals.

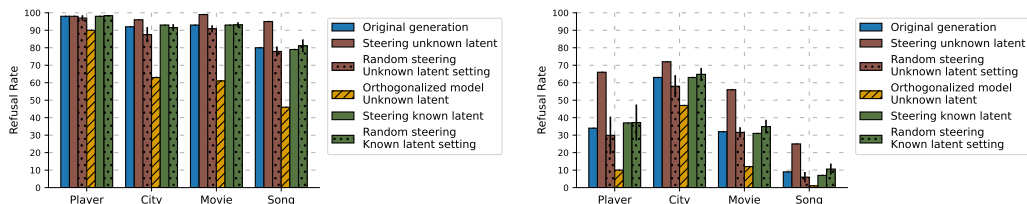


Figure 26: Number of times Llama 3.1 8B refuses to answer in 100 queries about unknown entities (left) and known entities (right). We examine the unmodified original model, the model steered with the known entity latent and unknown entity latent, and the model with the unknown entity latent projected out of its weights (referred to as Orthogonalized model). The mean and standard deviation of steering with 10 random latents are shown for comparison.

Further analysis reveal similar findings to those in Gemma regarding attention patterns: steering with the top known entity latent increases the attention scores to the entity (Figure 27 top), while unknown entity latent steering result in diminished attention scores (Figure 27 bottom).

The replication of our key findings—originally observed in Gemma—across Llama 3.1 8B strengthens our confidence in both our methodological approach and the broader applicability of our results. This generalization is particularly noteworthy given the substantial architectural differences between the two models and their respective SAEs.

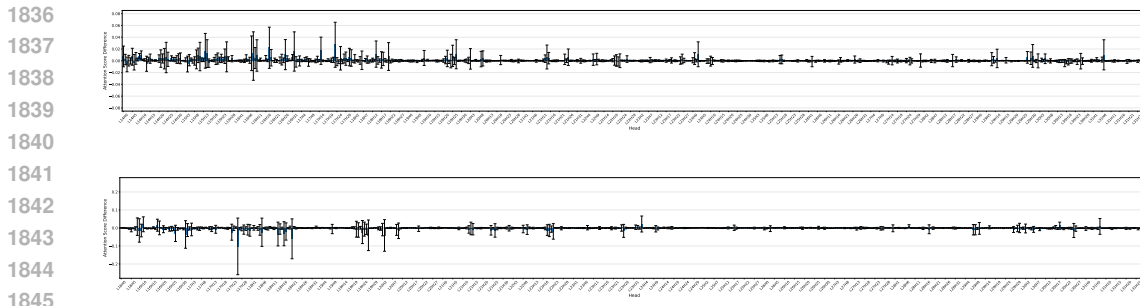


Figure 27: Aggregated attention scores to entity tokens per head in Llama 3.1 8B top known entity (top) and unknown entity (bottom) latents.

## R ACTIVATION FREQUENCY ON SONGS DATA AFTER KNOWLEDGE CUTOFF

Model	Known Entity Latent	Unknown Entity Latent
Gemma 2 2B	6%	53%
Gemma 2 9B	22%	55%
Llama 3.1 8B	13.4%	76%

Table 8: Activation frequency of each of the top known and unknown entity latents on songs released after knowledge cutoff (August 2024).

## S TOKEN LIKELIHOOD HYPOTHESIS

An alternative explanation for our observed entity recognition latents is the *token likelihood hypothesis*: the latents might simply encode token likelihood rather than actual knowledge about entities. Under this hypothesis, when processing a token sequence  $(t_1, \dots, t_{i-1}, t_i)$ , the activation of our discovered latents at position  $i$  could be explained by the model’s ability to predict token  $t_i$  from previous context. For instance, given a well-known movie title, the model would more easily predict subsequent tokens, potentially triggering what we interpret as ‘known entity’ latents. Conversely, for unknown entities, lower token likelihood might activate our ‘unknown entity’ latents. This represents a plausible confounding factor, as tokens comprising well-known entity names are inherently more predictable in the training distribution than those of unknown entities.

To test this hypothesis, we analyze token likelihood on a broad text corpus from the FineWeb dataset (Penedo et al., 2024). For each token position  $i$ , we compute both the entity recognition latent activations and the probability of the ground-truth token being predicted from position  $i - 1$ ,  $p(t_i|t_{<i})$ . If the token likelihood hypothesis were true, we would expect strong correlations between these measures.

Our analysis reveals several key findings that challenge this hypothesis:

- Entity recognition latents activate selectively, firing on only a small fraction of tokens (e.g. 0.6% for known entity latents and 0.5% for unknown entity latents in Gemma 2 2B, see Table 9).
- The correlations between latent activations and token prediction probabilities are negligible across all tested models (Figure 28).
- We explored various other potential relationships, including dependencies on the perplexity of surrounding tokens and next-token prediction entropy, finding no substantial correlations.

While we observe that tokens where unknown entity latents activate tend to have lower prediction probabilities compared to the baseline, this effect is modest given the latents’ sparse activation patterns. These findings suggest that token predictability alone cannot explain the behavior of our

entity recognition latents, supporting our interpretation that they encode a more sophisticated form of knowledge awareness.

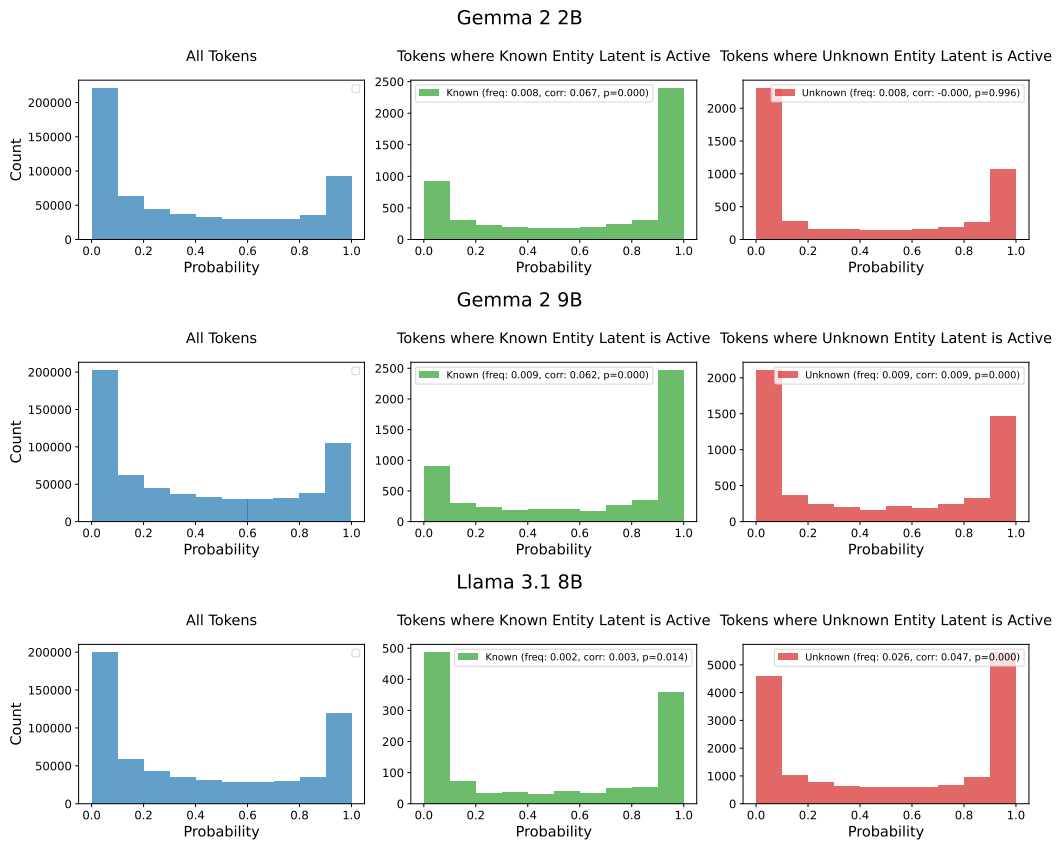


Figure 28: Distribution of ground-truth next-token probabilities for Gemma 2 2B (top), Gemma 2 9B (middle), and Llama 3.1 8B (bottom). For each model, we show three distributions: (left) across all tokens in the dataset, (middle) for tokens where the known entity latent activates, and (right) for tokens where the unknown entity latent activates.

Model	Latent	Activation Frequency	Correlation with $p(t_i t_{<i})$
Gemma 2 2B	Known	0.006	0.067 (p=0.000e+00)
	Unknown	0.005	-0.000 (p=9.960e-01)
Gemma 2 9B	Known	0.009	0.062 (p=0.0e+00)
	Unknown	0.009	0.009 (p=1.045e-12)
Llama 3.1 8B	Known	0.002	0.003 (p=1.380e-02)
	Unknown	0.026	0.047 (p=0.000e+00)

Table 9: Activation frequency and correlation with conditional next-token probability for top known and unknown entity latents in each model.